Journal of Population Therapeutics & Clinical Pharmacology

RESEARCH ARTICLE
DOI: 10.53555/jptcp.v30i18.3484

EFFECT OF SILYMARIN PARTICLE SIZE ON ITS SOLUBILITY ANDORAL BIOAVAILABILITY, THE ENHANCEMENT OF PHARMACOLOGICAL ACTIONS

Mujahid Sher[1,2], Ishtiaq Hussain[1], Farhat Ali Khan[3], Hamid Hussain Afridi[4], Wiaam Mujahid Sher[5], Naila Gulfam[6], Muhammad Saqib Khalil[7*], Akhtar Aman[8], Muhammad Sulaiman[9], Zeeshan Ahmad[10]

[1]Department of Pharmacy, Abbottabad University of Science and Technology, Abbottabad, Pakistan. Orcid.org/0000-0002-4594-9821. mujahidss.aventis@gmail.com
[1]Department of Pharmacy, Abbottabad University of Science and Technology, Abbottabad, Pakistan. drishtiaq025@aust.edu.pk.
[2]Premier Institute of Health Management Sciences, Peshawar, KP, Pakistan
[3]Department of Pharmacy, Shaheed Benazir Bhutto University Sheringal, Dir Upper 18000, Pakistan. farhatkhan2k9@yahoo.com.
[4]Department of Pharmacy, Shaheed Benazir Bhutto University Sheringal, Dir Upper 18000, Pakistan. hamid@sbbu.edu.pk
[5]Khyber Medical College, KP, Pakistan; wiaamsher16675@gmail.com
[6]Jinnah College for Women, University of Peshawar, KP, Pakistan nailazoo@yahoo.com
[7*]Sarhad University of Information Technology, Peshawar, Pakistan; saqib.biotech@suit.edu.pk
[8]Department of Pharmacy, Shaheed Benazir Bhutto University Sheringal, Dir Upper 18000, Pakistan. dramanrph@sbbu.edu.pk.
[9]Jiangsu Center for Pharmacodynamics Research and Evaluation, China Pharmaceutical University, Nanjing China. Email: drsulaiman66@gmail.com
[10]Department of Microbiology, Hazara University Manshera, Pakistan, zeeshanmicro100@gmail.com

[*]**Corresponding Author:** Muhammad Saqib Khalil
Email: saqib.biotech@suit.edu.pk

Co-corresponding Author: Mujahid Sher
Email: mujahidss.aventis@gmail.com

Abstract:
Due to the many side effects associated with conventional medicine, people turned their attention towards natural drugs, which have fewer or no side effects. However, their usesare restricted due to lower solubility and bioavailability. Plant-based nanoparticles have been demonstrated as more effective alternatives, and nanoparticles are reported to increase the bioavailability and solubility of natural medicines to make their better use. The nanotechnology system is innovative to enhance the therapeutic effects and bioavailability of naturally occurring drugs. Therefore, silymarin nanoparticles were prepared using two different methods. Characterization analysis confirmed the reduction in particle size and conversion to amorphous states.The achieved nanoparticles have the required size, optimum zeta potential, and PDI. Results from solubility and bioavailability studies are very encouraging. The prepared nanoparticles were tested for hepatoprotection; they proved better than the

unprocessed drug in terms of better effects on hepatic marker enzymes, serum total albumin and protein values, and hepatic histopathology. The prepared nano drug is recommended for clinical trials.

Keywords: silymarin nanoparticles; hepatoprotection; hepatic histopathology; albumin and protein values

1. Introduction

Medicinal plants have the potential to provide many benefits to society. They have many effects on humans and animals, like antiaging, antimicrobial, astringent, antipyretic, rubefacient, antispasmodic, blood glucose regulation, blood pressure regulation, and antiseptic effects, to name a few [4]. Acquiring plant drugs is cheap, efficient, simple, and easy to prepare. Plant medicines cause minimum side effects and may offer additional benefits compared to synthetic drugs. It may be surprising to learn that a natural product, synthetic component, or prototype entity derived from a natural product were all present in about half of the pharmaceuticals produced over the past two decades and subsequently approved by the US FDA [5].

Chemicals formed in medicinal plants, which are an element of their normal metabolic activities and are not involved directly in the growth process, are known as secondary metabolites. Alkaloids, flavonoids, phenolic compounds, and terpenoids all fit in the class of secondary metabolites [6]. Because secondary metabolites may resemble endogenous metabolites, hormones, or molecules that cause signal transduction, they frequently have curative and disease preventing effects. Scientific investigations have proven such benefits after the increased consumption of secondary metabolites [7]. Some important herbs that abundantly contain secondary metabolites include Silybum marianum, ginger, and capsicum, in which various useful phytochemicals have already been found.

Silymarin, isolated from Silybum marianum, belongs to the family Asteraceae. It is a naturally produced hybrid molecule derived biogenetically from flavonoids and lignans and known as a flavonolignan [8]. It is produced as a raw material for the pharmaceutical industry in Argentina, China, Hungary, Austria, Germany, and Poland. Silymarin is widely used to treat various diseases because of its safety and lack of side effects. It is a natural therapy for liver ailments, biliary tract disorders, diabetes, inflammation, hyperlipidemia, and many other health issues [9]. It has been usedextensively everywhere in clinical settings, including in the United States, to treat hepatotoxicity [10].It is a proven multifunctional compound [11] and is also used as a reference drug in evaluating potential hepatoprotective novel medicines [12].

Silymarin has significant antioxidant and cell regenerating capabilities. Its antioxidant action protects the cell membrane against damage caused by the peroxidation of polyunsaturated fatty acids (caused by free radicals) in the cell membrane bilayer, ultimately destroying hepatocyte components. It can also directly interact with cell membrane constituents to protect them from any irregularities in the lipid composition necessary for maintaining normal fluidity [13]. It can counteract the loss of SOD and GSH by lowering free radicals, boosting SOD and GSH levels, and inhibiting glutathione oxidation [14]. Silymarin enhances protein production at the ribosomal level [14] to restore the structural proteins and enzymes for promoting the regeneration of liver tissue. Silymarin can also regulate membrane permeability, control membrane integrity, and boost membrane stability against xenobiotic damage [15]. It can regulate nuclear expression through steroid-like effects due to its structural resemblance to steroidal hormones and can prevent stellate hepatocytes from evolving into myofibroblasts, the collagen fibers that cause cirrhosis [16].

Both in animal models and in human clinical settings, silymarin has been shown to have hepatoprotective activities [17]. It has demonstrated protective properties against hepatotoxic drugs used in tuberculosis in animal studies [18]. In a randomized controlled trial, silymarin administration effectively decreased the AST to platelet ratio and the fibrosis score, improving the histology of the liver [19]. Silymarin and the Mediterranean diet have significantly improved the glycemic profile and reversed liver injury [20]. Silymarin, vitamins C, E, and Q10 supplement has been shown to improve liver function histologically and reduce liver toxicity markers like ALT, AST, and ALP, as well as

lipid markers in NAFLD patients [21]. According to a different study, silymarin's antioxidant action is linked to its usage in treating hepatitis and cirrhosis [14]. Silymarin administration in rats has demonstrated an intense protective action against diazinon-induced liver damage [22]. Silymarin reduced ALT, AST, and ALP levels, and the rats had higher serum and liver tissue levels of superoxide dismutase. Likewise, it dramatically reduced the sinusoidal dilatation, intense vacuolization, and inflammation in hepatocytes near the central vein. An *in vivo* study showed that silymarin can restore normal levels of hepatic antioxidant enzymes and ameliorate cellular abnormalities induced by CCl4 intoxication.

Most importantly, compared to unprocessed silymarin, the silymarin phytosomal preparation significantly enriched silymarin per oral bioavailability and offered a 6 fold increased systemic bioavailability. According to the authors, this is a better alternative for natural drugs with poor aqueous solubility to improve their oral bioavailability [23]. Due to the increasingly wide use of strategies and techniques to enhance the bioavailability of this crucial product, silymarin nanoformulation has been tested in Erlich ascites. Compared to the unprocessed silymarin, nanoformulation substantially affected apoptosis and proliferation in tumour cells [24]. Silymarin can be a viable treatment alternative, especially when other medications are contraindicated or have failed, or it can be used in conjunction with other therapeutic agents as a complementary treatment [25].

2. Materials and Methods

PCSIR Peshawar provided silymarin as a gift for this study. Ethanol, methanol, DMSO, and n-hexane were purchased from BDH. Xylene was purchased from Lab-Scan, Ireland. From the neighbourhood market in Peshawar, healthy rabbits were obtained. Rats were bought from the NIH in Islamabad.

2.1. Fabrication of nanoparticles

Nanoparticles were prepared by two methods: The Evaporative Precipitation of Nanosuspension (EPN) and Antisolvent Precipitation with a Syringe Pump (APSP).

2.1.1. Evaporative Precipitation of Nanosuspension

We used methanol as solvent and n-hexane as antisolvent to fabricate the nanoparticles in this method. In the EPN technique, a silymarin-saturated solution was prepared in methanol. The solution was added quickly to n-hexane, which resulted in nanoparticle formation. During the mixing of solvent and antisolvent phases, stirring was continuously performed. The resulting mixtures were evaporated soon with the help of a rotary evaporator operating under a vacuum pump to obtain nanoparticles [30]. To acquire the best nanoparticles in terms of particle size, zeta potential, and PDI, the essential experimental conditions like stirring speed and solvent antisolvent ratios were optimized during the nanoparticle preparation process [31]. Different solvent-to-antisolvent ratios and stirring speeds were tried in separate experiments.

Stirring Speed was the first parameter that was optimized, and it was assessed between 1500 and 3000 rpm. The solvent antisolvent ratios were held constant while optimizing the stirring speed. We discovered that as the stirring speed increased, the particle size decreased. A stirring speed of 3000 rpm was recorded as the optimum stirring speed required to prepare nanoparticles with the desired features. While maintaining a constant stirring speed at 3000 rpm, solvent antisolvent ratios were also optimized to control the synthesized nanoparticles' sizes further.

The solvent antisolvent ratio is also essential and can impact the size of prepared nanoparticles. It was the second parameter we optimized after the stirring speed in fabricating nanoparticles by the EPN method. As the solvent-antisolvent ratio is increased, the particle size decreases [31], and the drug quickly precipitates into nanoparticles when its solution is mixed into the antisolvent. Additional antisolvent will result in a greater nucleation rate and smaller nuclei. Diffusion distance for growing species grows, becoming the limiting step for the growth nucleus as the antisolvent concentration rises in the subsequent growth [32,33]. The ratios for solvent and antisolvent were assessed from 1:20 to 1:10 while maintaining the stirring speed constant.

2.1.2. Antisolvent precipitation with a syringe pump

According to the APSP approach, unprocessed silymarin was soluble in 50 mL of ethanol before being delivered into the antisolvent phase. Silymarin solution was filled in the syringe and immediately introduced into a certain volume of n-Hexane (antisolvent) with a 2 mL/min flow rate and was continuously stirred throughout the process. The nanoparticles were obtained by quickly evaporating the resulting nanosuspension with the help of a rotary evaporator operating under vacuum[30]. To acquire nanoparticles possessing the best features, essential parameters during the nanoparticle preparation process, like stirring speed and solvent antisolvent ratios, were optimized [31]. The optimized stirring speed and solvent-to-antisolvent ratio were selected, which resulted in the preparation of nanoparticles of the required size and shape.

The synthesis of nanoparticles using the APSP technique involved optimization of the experimental conditions. The stirring speed was assessed between 1500 and 3000 rpm, during which solvent antisolvent ratios were held constant. It was learned that increasing the stirring speed led to a decrease in particle sizes. While maintaining a constant stirring speed of 3000 rpm, solvent antisolvent ratios were also optimized to control the synthesized nanoparticles' size further.

The solvent-antisolvent ratio is significant because it can affect the size of nanoparticles. As the solvent antisolvent ratio is increased, the particle size decreases. The drug quickly precipitates into nanoparticles when the solution of the drug is added to the antisolvent. The solvent-to-antisolvent ratios were assessed from 1:20 to 1:10 when the speed of stirring was constantly maintained at 3000rpm. The sizes of the drug particles were found to drastically reduce when the solvent-antisolvent ratio was increased [31].

2.2. Assay of the prepared nanoparticles

The prepared nanoparticles were analyzed for drug content. The method previously described was used to determine the sample content [34]. Methanol was used to make a standard sample solution with an end concentration of 0.033mg/mL. To prepare the stock solution for the sample assay test, 33 mg of the sample was dissolved in a 100 mL volumetric flask. It was sonicated for 5 minutes after 70 mL of methanol had been added. Methanol was also used to raise the final volume to the desired level after sonication. After thorough mixing, it was filtered through a syringe filter of 0.02 µL bore. After filtering, the solution was further diluted with methanol to a 0.033 mg/mL concentration. It was then measured for silymarin at 286 nm with a spectrophotometer. Methanol was the blank used in this experiment. The results of the investigation were acquired in triplicate.

2.3. Characterization

The prepared nanoparticles were characterized using modern characterization techniques such as Scanning Electron Microscopy, FTIR, XRD, Zeta Sizer, and DSC. The characterization techniques used in this experiment can give reliable results for such products.

2.3.1. Scanning electron microscopy (SEM)

In this research work, JOEL JSM-5910, Tokyo, Japan, was employed to obtain samples of electron micrographs. The scanning electron microscopy technique uses electrons in its place of light to form an output image [35]. Electrons are reflected when incident light contacts the sample surface and are drawn to a detector, where an algorithm transforms them into pictures. Varying accelerating voltages and magnifications were used to attain the requisite micrograph resolution. A few sample droplets were applied to the instrument's metallic stub using double-sided adhesive tape and were vacuum dried before that for analysis. During the analysis, the system's working voltage stayed at 30 mA for two minutes while the accelerating voltage stood at 20 kV.

2.3.2. Analysis with Zeta Sizer

Malvern Instruments, UK, Nano series ZS 90, regarded as a suitable instrument for such analysis, was used to characterize the particles for sizes, polydispersity index, and zeta potential. This method can

measure particles between three nanometers and three micrometers in size. A fundamental component of zeta-sizer analysis is to measure fluctuations in the strength of scattered light caused by random particle movement. Ultra-pure water was supplied to the nanoparticles while the system temperature was held at 25 ℃ to obtain the proper scattering intensity for analysis. Before analysis, the samples were dispersed well in the aqueous medium with ultrasonication. Ultrasonication helps to maintain the polydispersity index below 0.5, which is required during analysis. Nanoparticles of the samples were introduced to a specifically developed cuvette with the help of a micropipette to perform the analysis.

2.3.3. X-ray Diffraction (XRD)

X-ray diffractometer, "The PANalytical X'Pert Pro (PANalytical, Almelo, the Netherlands)," was employed to collect the XRD pattern of unprocessed drug and drug nanoparticles. XRD can validate the crystalline form of a matter and any changes in that form. XRD is a quick, nondestructive analysis method that scarcely requires sample preparation. The sample holders were made of silicon for the nanoparticles, and a plastic sample holder was employed for the unprocessed drug. The machine was set to 40 kV voltage and an operating current of 30 mA. Angles of 5° and 40° were chosen as the initial and final angle points at 2θ. Throughout the procedure, each step's size and duration were 0.02o and 0.5 seconds, respectively [36].

2.3.4. Differential Scanning Calorimetry (DSC)

Mettler Toledo 822e (Greifensee, Switzerland) was utilized to conduct DSC investigations for all the samples. By Differential Scanning Calorimetry tests, we can assess the effects of particle size reduction on the thermal kinetics of the unprocessed drug and manufactured nanoparticles. A comparison of the enthalpy (ΔH) of the original sample and its corresponding nanoparticles yields information about the crystallinity [37]. 5mg of each sample was put separately in an aluminium-made pan in the sample chamber for analysis. As a reference, an unfilled pan (having no sample) was also used. The pans were heated at 10°C per minute between 60 and 200ºC while exposed to nitrogen gas flow at a 40 mL per minute rate [37].

2.3.5. Fourier-Transform Infrared Spectroscopy (FTIR)

This technique identifies any potential interactions between the drug and the excipients used to prepare the nanoparticles. In the current research work, Shimadzu IR Prestige-21 FTIR, Kyoto, Japan, was employed. The spectra were collected between 4000 and 400/cm. The sample was made by mixing 200–300 mg of potassium bromide (KBr) with 2–3 mg of the sample and then compressed with a compression machine to prepare transparent discs that were put in a sample container and examined. The component compatibility of nanoparticles was determined by matching the nanoparticle peaks and patterns to those of unprocessed drugs.

2.3.6. Spectrophotometric analysis

To calculate the per cent dissolution and solubility and conduct content analysis, PharmaSpec 1700, Shimadzu Tokyo, Japan, was utilized. The analysis was performed at the appropriate "ʎmax" (286 nm for silymarin in this study) after the sample and reference standards had been diluted [38].

2.4. Solubility study

A solubility study was performed for the unprocessed silymarin and its nanoparticles. The extent of the solubility of the Nano forms was compared to the unprocessed drug. To determine solubility, 200 mg of unprocessed silymarin and its nanoparticle form were transferred separately to 25 mL volumetric glass flasks and mixed with a known quantity of distilled water. The said volumetric flasks were sealed with aluminium foil to prevent loss from the evaporation of the solvent. The flasks were positioned in the orbital shaker for 24 h. The orbital shaker was fixed at 100 rpm and adjusted to 25 °C temperature. Following that, the samples were left undisturbed for 72 hours. The supernatant layer

was filtered with a Syringe Filter (0.02 µm, Whatman nanotop) so that any drug component that had not yet dissolved (≤ 0.02 micron size) could be retained on the filter and separated from the drug component that had dissolved. Following filtration, it was analyzed using a spectrophotometer at 286 nm to determine the solubility of silymarin [39]. The results of the analysis were obtained in triplicate.

2.5. Dosage form formulation

The next step was to formulate silymarin nanoparticles into a suitable dosage form, for which hard gelatin capsules were selected as the silymarin dosage form due to their processing simplicity. Its preparation involves only a few operations, like adding the medicine to the capsule body and sealing the cap to its body.

Silymarin has a very bitter taste, and this dosage form can significantly conceal its unpleasant taste. Lactose was employed as a diluent to change the ingredient mass to fit a size "3" capsule. Each capsule of unprocessed silymarin and its corresponding nanoparticles was manufactured by combining 50 mg silymarin with 100 mg lactose. Immediately following mixing, capsules were manually poured into their shells and sealed.

2.6. In Vitro release study

A paddle apparatus (Apparatus II) method was used for this experiment. This device uses a coated paddle that can reduce turbulence produced by stirring. A motor with changeable speeds revolves at a controlled speed while the paddle is vertically attached. The dissolution flask has a circular bottom, which reduces turbulence in the dissolution medium when the sample is put inside. The equipment is housed in a water hall with a temperature kept constant at 37 0C. The steps involved in this method are given below.

2.6.1. Sample preparation for the study

Tests for silymarin and its nanoparticle capsules were conducted separately following USP [40]. Apparatus II (USP) of six vessels (DT-80, Erweka, Germany) was utilized for the experiment. 900 mL of distilled water, pH 6.5, was added to each container. Its temperature was set at 37 ± 0.5 °C and operated at 100 rpm. Each dissolution vessel received one capsule. Five milliliters of dissolution media were drawn from each vessel at 10, 20, 30, 40, 50, 60, 70, 80, and 90 minutes and filtered through a 0.02 µm syringe filter. This was constantly changed out for new dissolution media to keep sink conditions consistent. After filtration, the sample was diluted to 100 mL using distilled water and mixed. The samples were diluted until a final 22.22 µg/mL concentration was obtained.

2.6.2. Standard preparation for the study

A standard stock solution of silymarin containing 0.225 mg/mL in methanol was produced in a 100 mL volumetric flask for the dissolution study. Using water with a pH of 6.5 as the blank, the samples and the standard spectrophotometric absorbance were measured at ʎmax of 286 nm. The formula below was used for calculating the drug release percentage.

$$\%\ Dissolution = \frac{Abs.of\ sample \times Weight\ of\ standard \times 5 \times 900 \times 50}{Abs\ of\ Std \times 100 \times 100 \times label\ claim \times 10} \times 100 \quad \text{Equation-I}$$

2.7. Stability study

Silymarin nanoparticles were tested for storage stability in a stability chamber. The stability was measured at temperatures ranging from 5 to 45 °C and at different pHs ranging from acidic to basic (1 to 9 on the Sorenson scale). The nanoparticles were also stored at pH 6.5 and 25 °C and checked for stability at intervals of days 1, 30, 60, 90, 120, 150, and 180. The labelled lots were periodically examined for polydispersity index, particle size, and aqueous solubility to determine the potential effects of temperature, pH, and time length on their stability.

2.8. Bioavailability study

Silymarin nanoparticles were tested for their bioavailability using a reported [41] method and compared with the bioavailability of the unprocessed compound. Two groups of six rabbits each were randomly made out of the study animals. The animals were strictly compliant with the recommendations the concerned body set. Following the chalked plan, oral gavage was used to provide 50 mg/kg of unprocessed silymarin or SM-APSP 50mg/kg b. w. to each animal. The first group was treated with unprocessed silymarin, and the second group received SM-APSP. Rabbits were fasting for 12 hours, with unlimited water access, before receiving samples. They wererestrained within the animal facility and had one ear closely clipped and cleaned with a pad of 70% isopropyl alcohol. After that, a vein in the outer ear was used to draw two milliliters of blood at specified time points of "0" hours (pre-administration), 1hours, 1.5hours, 2hours, 4hours, 6hours, 8hours, 12hours, and finally at 24hours. Using the reported procedure [41] [Wu,J.W.,2007], the bloodcentrifugation was performed instantly at 3,000g for twenty minutes, and the serum was kept stored as frozen (not for very long) until further examination with a UV-visible spectrophotometer. Blood samples were collected weekly following the same procedure, alternating the ears. Every test was conducted in triplicate.

2.9. Hepatoprotective activities

The Animal Ethics Committee of AUST, the body overseeing such operations, approved using the animals in all experiments. Male Wistar albino rats weighing (200 ± 20 g) were indiscriminately allocated into 5 equal groups (1-5), having six rats in each class. Each group was allocated to separate cages and labelled accordingly. Seven days of acclimatization were allowed. As a positive control, Group 1 contained healthy, untreated rats. Groups 2-5 were injected with CCl_4 to induce hepatic injury. As a negative control, group 2 received only injections of CCl_4 without treatment with silymarin samples. Group 3 was treated with unprocessed silymarin 200 mg/kg b.w. The leftover groups (4 and 5) received therapy with SM-APSP in various doses using oral gavage.

2.9.1. Hepatic damage induction

Intraperitoneal injections were given twice a week at premeditated doses of 2mL/kg b.w. of a 50% solution of CCl_4 in liquid paraffin to cause hepatic injury in rats. [42].

2.9.2. Determination of serum biochemicals

To confirm the hepatoprotective effects of silymarin, biochemical tests on the blood of rats were carried out every 2, 4, and 6 weeks. They were anaesthetized, and 2 mL of blood was drawn by cardiac puncture from every experimental rat and transferred into labelled tubes. Samples were made to spin to separate maximum serum. The collected serum was kept at 4°C until it was used forthe standard test procedures to measure the parameters of the liver function tests (LFT).

To determine alkaline phosphatase, the sample and reagent were combined, and the initial absorbance at 405 nm and start time were noted. The absorbance was re recorded after 1, 2, and 3 minutes.

U/l = 3300 × ΔA 405 nm/min Macro.

U/l = 2760 × ΔA 405 nm/min Semi-micro.U/l = 2760 × ΔA 405 nm/min Micro

To determine alanine transferase, 100 µL from the sample was mixed with 1000 µl of mono reagent, and its absorbance was observed at 340 nm after 1 min. The absorbance was noted again after 1, 2, and 3 minutes. The values of absorbance per minute were calculated to get ALT concentration (IU/L), multiplied with factor 1745

Aspartate transaminase assay was performed using the Cobas C111 automated Chemistry analyzer following the instructions given by the manufacturer [43].

All of the components were thoroughly mixed before measuring the sample and standard's absorbance at 600 nm in comparison to a blank for the determination of serum albumin.

Serum Albumin Concentration = Absorbance of sample/Absorbance of standard × Standard concentration To find out the serum concentration of total proteins (TP), all the contents were mixed

well and incubated for 30 min at 25 °C. Then, the absorbance of the sample and the standard against the reagentblank at 546 nm was noted to measure the serum concentration of TP.
Concentration of total protein = Absorbance of sample/Absorbance of standard × Concentration of Standard

2.9.3. Histopathological examination

After the experimental period ended, rats were fasted overnight and cervically dislocated the next day, immediately dissecting out their livers. Some liver tissue was placed in formalin (10%)immediately to conduct histopathological investigations. The liver tissue was washed with tap waterand dehydrated with alcohol ethyl solutions of 50%, 70%, 80%, 90%, and twice with 100% solution.The samples were washed with 100% xylene before being embedded in paraffin and heated to 50°C for 24 hours in a hot air oven. Tissue sections with a 4 μm thickness were cut by sledge microtome and placed on slides made of glass. After deparaffinization and staining with eosin and hematoxylin,the prepared slides were used for histopathological analysis [44]. They were examined under a microscope (Olympus, Japan) at 100 times magnification for histopathological changes.

3. Results and Discussion

There have been extensive investigations into silymarin for the treatment of various disorders. However, this treasurable drug has very poor water solubility, presenting serious challenges because its slow and incomplete dissolution results in insufficient oral bioavailability. Therefore, scientists spent a lot of time to develop new formulation strategies to address these issues. The objective of the current research was to prepare silymarin nano-sized particles by two separate techniques to enhance its solubility and associated oral bioavailability.

3.1. Fabrication of nanoparticles

3.1.1. Evaporative precipitation of nanosuspension (EPN)

According to the EPN approach and after following the optimization requirements for this method, nanosized particles were obtained with stirring speeds of 3000 rpm and a solvent antisolvent ratio of 1:10. At the fulfilment of these conditions, the EPN method provided silymarin nanoparticles having an average size of 161.19 ± 1.91 nm (Table 1).

Table 1. Particle size, Zeta potential, and PDI of SM-APSP

Method used	Average size ofparticles (nm)	Zeta potential(mV)	PDI
SM- APSP	69.12 ± 0.38	-33.4 ± 1.2	0.231 ± 0.01
SM-EPN	161.19 ± 1.91	-24.4 ± 0.81	0.122 ± 0.1

Table 2. Drug content unprocessed silymarin and SM-APSP

Product	Result
Unprocessed silymarin	95.61 ± 0.49%
SM-APSP	98.82 ± 0.46%

3.3. Characterization

3.3.1. Scanning Electron Microscopy (SEM)

In the SEM analysis, the morphology, sizes, and size distribution of synthesized nanoparticles of silymarin were investigated, and pictographs were recorded. Figure 1 shows the SEM pictographs of silymarin nanoparticles prepared by the APSP method. The white dots in the figure represent the acquired nanoparticles. The pictographs reveal that the synthesized nanoparticles exhibited a predominantly spherical shape and a reduced particle size. The nanoparticles have an average diameter of 69.12 ± 0.38 nm (Table 1).
The nanoparticles prepared by the EPN method (SM-EPN) were also subjected to SEM analysis, and a reduction in the size of the particles was noted. The results show that silymarin nanoparticles

prepared using the EPN method had an average particle size of 161.19 ± 1.91 nm (Table 1). According to the SEM pictograph, these nanoparticles, did not have even sizes; they were present as bunches and offered a broad size distribution [Figure 1(b and d)], unlike the nanoparticles prepared by the APSP method [Figure 1(a and c)].

As reported previously [39,45], with the size reduction, the surface area of the nanoparticles greatly increases, which can enhance their solubility, dissolution rate, and the associated oral bioavailability.

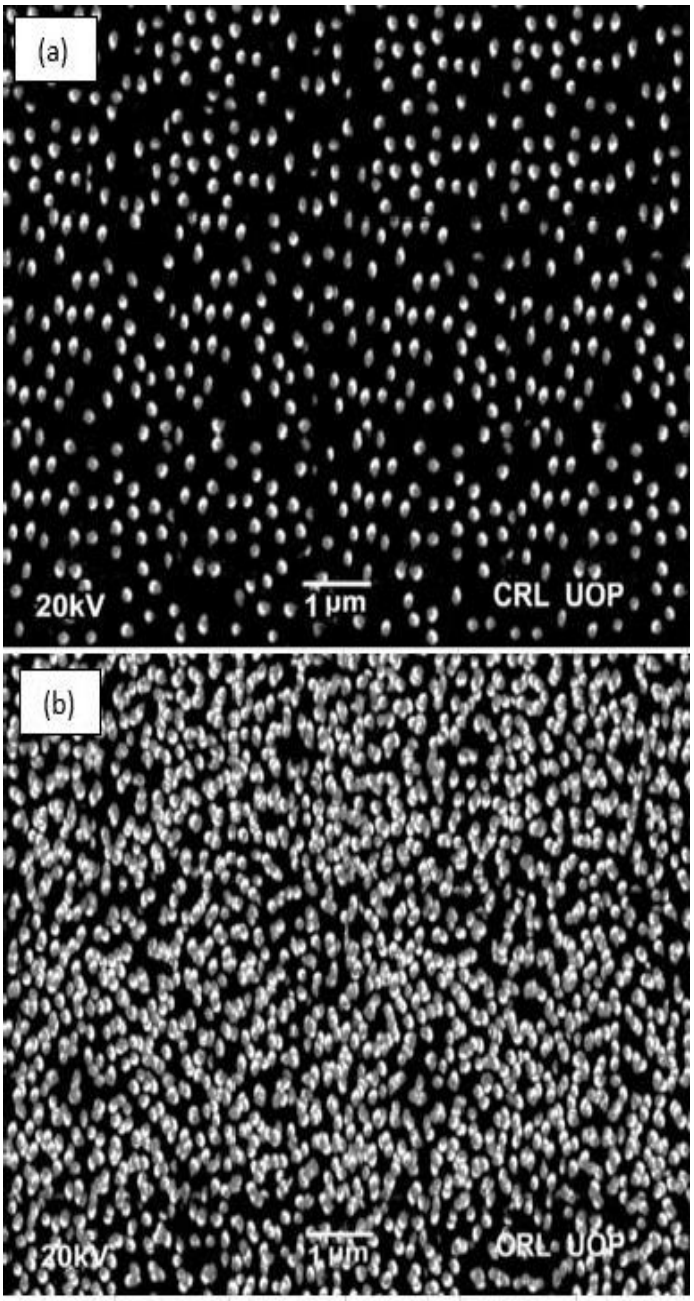

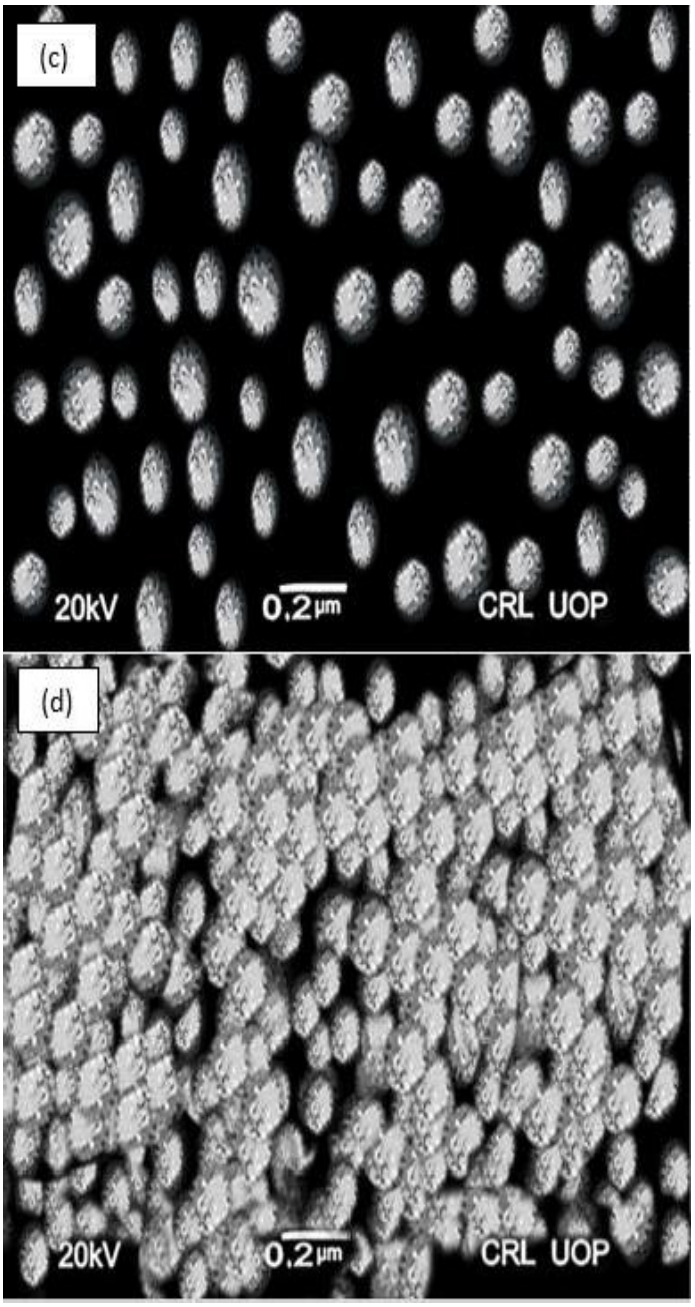

Figure 1. SEM pictographs of SM-APSP (a, c) and SM-EPN (b, d)

3.3.2. Analysis by Zeta Sizer

The dynamic size and surface potential of the synthesized nanoparticles were also determined. The results given in Table 1, represent the zeta potential (-33.4 ± 1.2 mV), polydispersity index 0.231 ± 0.01, and mean particle size (69.12 ± 0.38 nm) of silymarin nanoparticles. When the EPN method was used, we achieved nanoparticles having a zeta potential of -24.4 ± 0.81 mV, their polydispersityindex was noted as 0.122 ± 0.1, and their average particle size was noted to be 161.19 ± 1.91 nm (Table1).

The magnitude of zeta potential can be utilized to predict nanoparticle stability. Strongly charged particles with high zeta potential values promote redispersion and prevent aggregation due torepulsive forces, whereas weakly charged particles with low zeta potential may do the opposite [46].As a general rule, $\geq$ 30 mV and $\leq$ 60 mV values are considered good and excellent for stability, respectively [46]. Therefore, a zeta potential of -33.4 ± 1.2 mV indicates monodisperse nanoparticles without aggregates.

Other than zeta potential values, the nanoparticles size can also affect the crucial characteristics of pharmaceuticals like the release kinetics of the formulation and drug distribution. SM-APSP have

nanosized particles, which is very important because a reduction in particle size enlarges the surface area and the surface free energy of the particles. These factors are important for enhancing the dissolvability and release rate of drugs, which in turn leads to an enhancement in the drug's bioavailability and pharmacological actions [47].

In the case of the APSP method, the PDI value below 0.50 indicates even-sized particles. The nanoparticles also possessed anticipated and optimum zeta potential values (Table 1). The zeta potential of nanoparticles at these values means a greater repulsive force that will help avoid agglomeration of the prepared nanoparticles and promote their stability. Therefore, the prepared nanoparticles will have a longer shelf life.

3.3.3. X-ray Diffraction (XRD)

X-ray diffractometry analysis was conducted for silymarin in the unprocessed form and also after converting it to nanometer size. The XRD analysis of unprocessed silymarin demonstrated intense and pointed diffraction peaks at 2θ of 11.75º, 23.8º, 26.25º, 26.85º, and 28.29º. The presence of such characteristic peaks depicts a crystalline state (Figure 2b). The XRD analysis of silymarin nanoparticles showed their semi-crystalline form, as they revealed weaker diffraction peaks with reduced sharpness (Figure 2a). Such peaks, indicate decreased crystallinity and prove that SM-APSP is present in an amorphous state (Figure 2a). As established, the reduced intensity in the diffraction peaks is a feature of the reduced crystallinity of nanoparticles [48].

Silymarin melted at around 166 °C, and this is consistent with previously reported results [49]. SM-APSP exhibited a melting point at around 162 °C. The analysis undoubtedly validated the reduction in the crystalline nature and conversion of silymarin to an amorphous form.

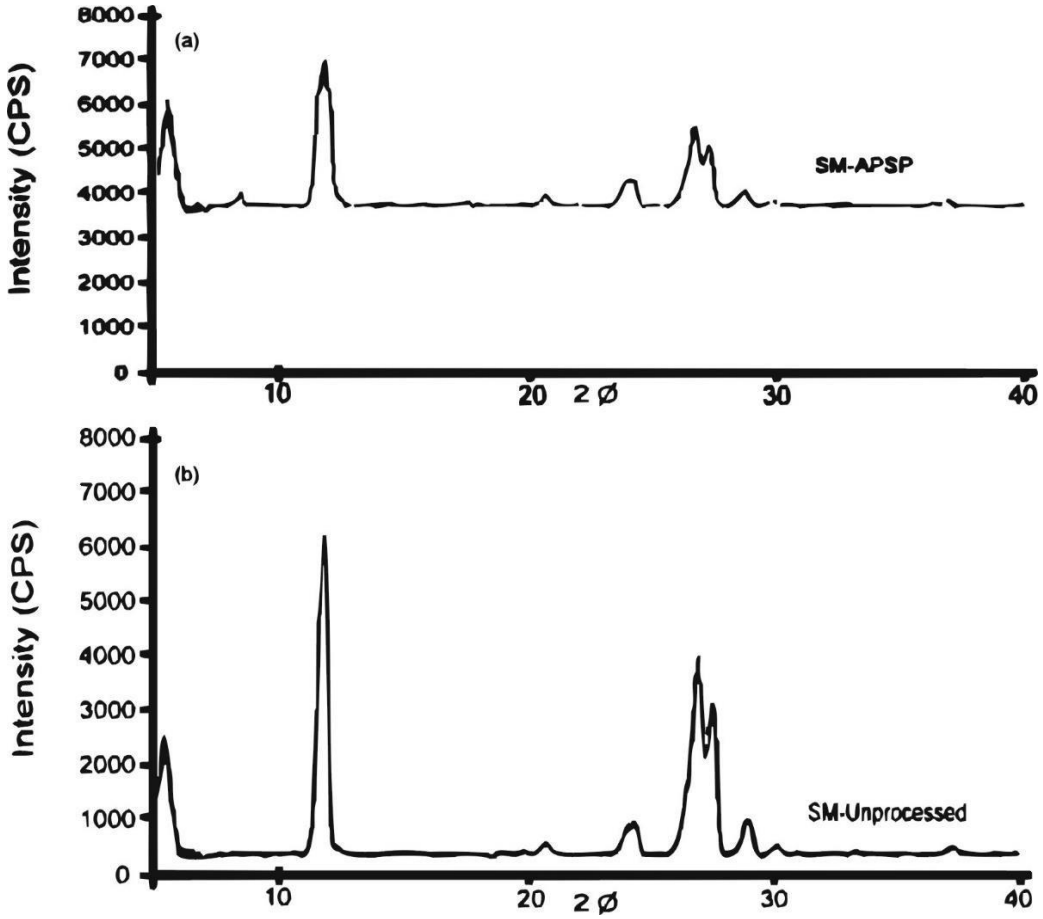

Figure 2. XRD diffractogram of SM-APSP (a) and SM-unprocessed (b)

Converting compounds to an amorphous state increases their solubility and improves their release rate, which ultimately enhance their bioavailability [50]. In contrast to crystalline materials, amorphous materials have higher free energy, therefore, they are efficiently soluble [51]. We can say that a change in crystallinity and conversion to nanometer sizes stand as the best approach to augment the drugs' solubility and dissolution, which increase their bioavailability [52].

3.3.4. Differential Scanning Calorimetry (DSC)

This approach is utilized for thermal analysis of a wide range of materials. DSC tests evaluated the effects of particle size reduction on the thermal kinetics of the prepared nanoparticles. The results obtained during the calorimetric analysis are shown in Figure 3. An expansion in the breadth and a slight decline in the elevation of the melting point peak can be noticed when the amorphous form of the compound is analyzed (Figure 3).

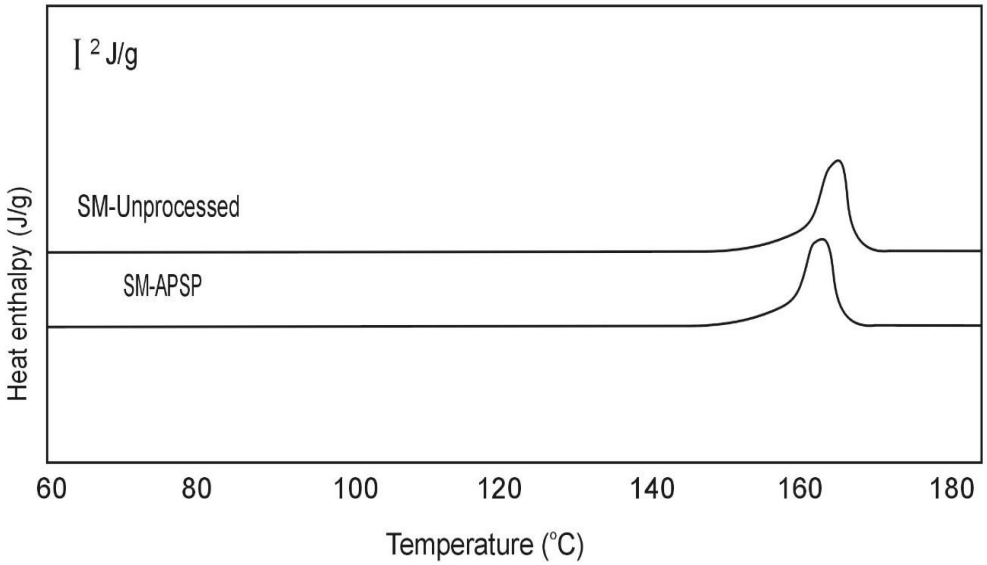

Figure 3. DSC Analysis Results of unprocessed silymarin and SM-APSP

In the DSC analysis of the samples (Figure 3), a clear endothermic peak (representing the crystallinity of the material) was detected at melting point temperature (166ºC) for unprocessed silymarin, whereas the SM-APSP displayed a melting point slightly lower than that required for the unprocessed drug. A lower acute melting point associated with silymarin in the nanoparticle state (the amorphous or semi-crystalline state) is due to the nanoparticles' low packing density. Since the peak observed in the case of SM-APSP was wider and not as sharply centered compared to that of unprocessed silymarin, it is clear that silymarin crystallinity decreased after being converted to nanoparticle form.

The decrease in melting point may be ascribed to the conversion of the drug to an amorphous form, the reduced particle size, and surface area, the major parameters that significantly influence the melting point temperature [38]. The melting point temperature denoted by "Tm," is greatly influenced by the particle size and surface area. When the lattice of a crystal breaks down owing to heat, an endothermic process is shown by the steep peak that is produced in the melting point region of the crystal.

The enthalpy of fusion (ΔH) value is another metric that indicates whether a material is crystalline or not. Crystalline materials have higher ΔH values, and less crystalline materials or amorphousmaterials have lower enthalpy values compared to their respective unprocessed compounds [53]. Theenthalpy (ΔH) values of the unprocessed silymarin sample and the nanoparticles form were also compared to determine the crystalline nature of the samples [54].

3.3.5. Fourier-Transform Infrared Spectroscopy (FTIR)

FTIR analysis was conducted for both samples of silymarin. The FTIR spectrum is helpful for the identification of our samples and the comparative evaluation of their vibrational frequencies. The vibrational changes in the materials are determined by the intermolecular interactions. The investigation points towards a spectrum obtained with many peaks of changeable intensities due to vibrational fluctuations that represent different functional groups. The infrared spectra of silymarin (unprocessed) and SM-APSP using Fourier transform infrared spectroscopy are displayed in Figures 4a and 4b. The figure shows that all functional groups vibrate at specific frequencies, which are visible in the FTIR spectrum as distinct peaks of varying intensities [55]. The results of the FTIR analyses of all the samples show that the chemical makeup of the sample in nanoparticle form is quite comparable to that of the sample in its unprocessed form. The analysis confirmed that no new complex had developed within the constituent parts of silymarin, and the fabricated nanoparticles still have their structural integrity.

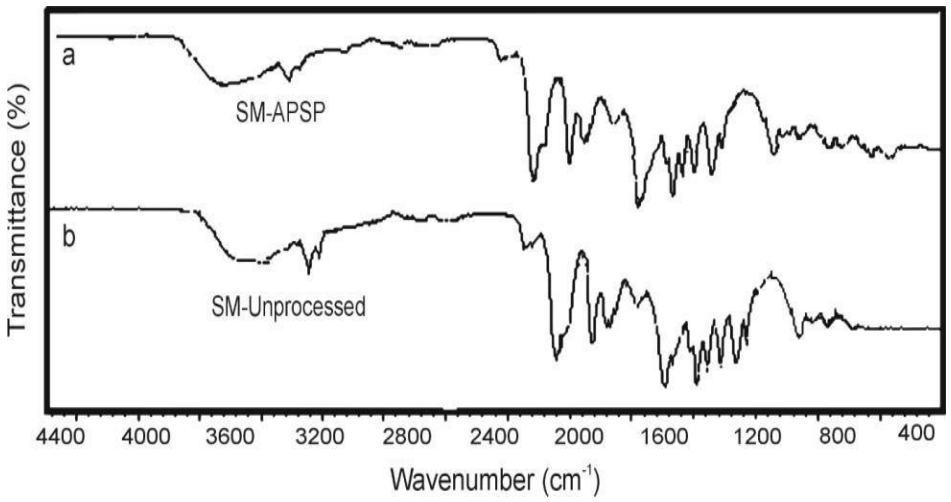

Figure 4. FTIR spectra of SM-APSP (a) and SM-unprocessed (b)

3.4. Solubility study

A solubility study was performed to determine the maximum solubility and enhancement in the solubility of the prepared nanoparticles. Figure 5, given below displays solubility data acquired from unprocessed and nanoparticle forms of silymarin in distilled water. It is clear from the data that the aqueous solubility of the nanoform of silymarin greatly increased in comparison to the solubility of the drug that was not processed. SM-APSP solubility was noted at 413.3 ± 02.31 µg/mL (Figure 5) as compared to the solubility of unprocessed silymarin (221.4 ± 3.2µg/mL).

When compared to the unprocessed compounds, the aqueous solubility of the nanoparticles of the drug (SM-APSP) increased greatly. The transformation of the drug into an amorphous state and its transition into nanosized particles, leading to an increase in the drug surface area, its wetting capacity, and surface free energy, can all explain improved solubility of SM-APSP. All the processes can collectively enhance the dissolvability and rate of release of the drug immensely [39,52]. Reduction in the crystallinity or conversion to amorphous form, as established in the DSC studies, and reducing the particle size to the nanometer range are the foremost causes of the enhanced solubility of the drugs in nanoparticle form [52]. In comparison to the unprocessed drug, the nanoform possesses extra surface-free energy, which is also an essential factor for solubility enhancement. The increased solubility of silymarin after the transformation into an amorphous state is because the solubility of less crystalline compounds is greater than that in the crystalline state (unprocessed) [39,52].

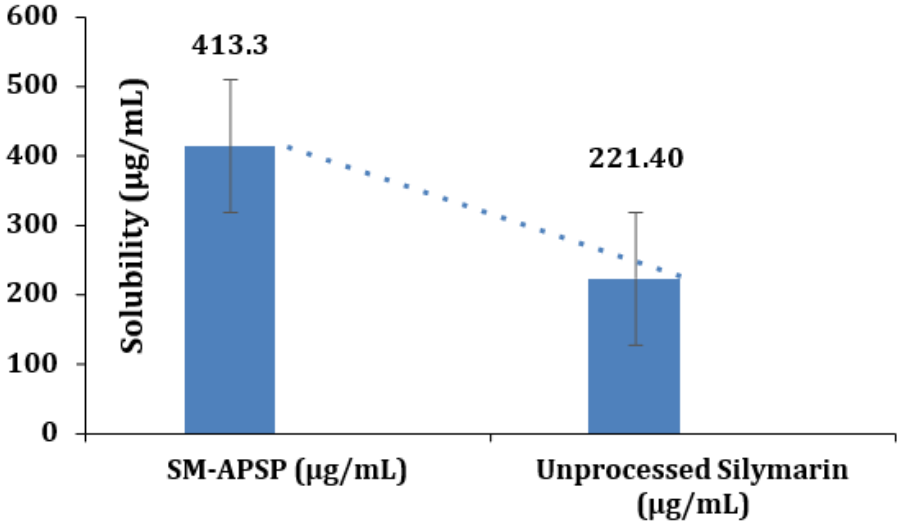

Figure 5. Aqueous solubility (µg/mL) of unprocessed silymarin and SM-APSP

3.5. In vitro dissolution study for unprocessed silymarin and SM-APSP

To evaluate a drug's performance, its dissolution rate must be measured. This experiment for unprocessed drug and SM-APSP was performed in distilled water at pH 6.5. The data from the dissolution study demonstrates that the dissolution of SM-APSP is far better compared to unprocessed silymarin in the same medium for a similar duration.

Table 3 below, shows the dissolution pattern of unprocessed silymarin and SM-APSP. The sample withdrawn after the first 10 minutes from the respective vessels contained 16.86 % silymarin from the nanoform of capsules, compared to the 4.91 % of silymarin released from the capsules of the unprocessed drug. A similar trend persistently followed, and after 30 minutes, 80.102 % dissolution of the SM-APSP and 19.104% of the unprocessed drug was recorded. Finally, at 90 minutes, 100.0% of the SM-APSP and just 39.99% of the unprocessed drugs were dissolved (Table 3). The data showed an enhanced dissolution of SM-APSP compared to unprocessed silymarin.

Table 3. *In vitro* dissolution profile of unprocessed silymarin and SM-APSP at pH 6.5

Time(min)	SM-APSP	Unprocessed silymarin
	(% of drug dissolved)	
0	0.00	0.00
10	32.34	15.11
20	53.48	23.22
30	70.11	28.12
40	80.22	36.10
50	95.89	39.51
60	100.00	44.12
70	100.00	44.94
80	100.00	45.21
90	100.00	45.66

Since nanoparticles make available a larger surface area for wetting in comparison to unprocessed drugs, the dissolution of drugs in the nanoform is enhanced. According to the Noyes-Whitney and Ostwald-Freundlich equations, the huge surface area of nanoparticles accelerates both the kinetics of dissolution and saturation solubility. Because of the huge surface area, the drug is released more quickly, taking less time to reach greater drug concentrations at the absorption site. All these factors improve the drug's absorption rate and, ultimately, its bioavailability.

The enhancement in the rate of dissolution is a primary characteristic of nanoparticles materialized due to definite reasons, such as conversion to an amorphous state, diminished aggregation among particles, expansion in the superficial area, and better wettability [56]. Due to improvement in the drug's gumminess to the cell membrane caused by the nanoparticles' small sizes, the bioavailability of poorly water-soluble drugs can vastly increase [57]. Since solubility and dissolution are the rate-limiting processes for a given drug, it is critical to address the problem of poor aqueous solubility of important medicinal compounds like silymarin. The improved dissolution rate of silymarin, shown in the current investigation, can predict an improved and faster rate of absorption and superior

bioavailability [58]. After conversion to the nano form, the particles' surface area increased and the diffusion layer got thinner, which led to a far better dissolution [59].

The fundamental goal of preparing nanoparticle versions of medications with low bioavailability is to speed up their dissolution, which will, at the end of the day, improve their bioavailability, and the dissolution rate is in a straight line related to the surface area [60]. The solids' rate of dissolution is explained by the equation presented by Nernst-Brunner (Equation-II):

$$\frac{dM}{dt} = \frac{\upsilon s}{Vh}(Cs - C) \quad \text{Equation-II}$$

According to the equation, a size decrease alone can increase the drug release rate while maintaining equivalent physical features [61]. Large particle sizes of unprocessed drugs lead to lower water solubility and a slow rate of dissolution, leading to lesser permeation of the drug particles [62].

An enhanced pharmacological effect of a drug is possible if the drug reaches in larger amounts to the areas where its effects are needed [38]. More drug release leads to enhanced drug concentration at the site of action; therefore, SM-APSP may be recommended as a better alternative if there is a need to produce an enhanced pharmacological action even with a smaller dose.

3.6. Stability study

The stability of a drug formulation has a critical part to play in the procedures of drug development, transportation, and long-term storage. Therefore, according to the International Organization of Standardization (ISO) defined guidelines, silymarin nanoparticles were tracked to check their physical stability. Various essential parameters related to the drug stability, like dissolution rates, thedrug content (percentage of drug), the physical appearance of nanoparticles, and average particle sizesof prepared nanoparticles, were periodically monitored. While analyzing the effect of pH on nanoparticle stability, their temperature was kept constant at 250C, and when testing temperature stability, the pH was kept constant at 6.5. The results of nanoparticle stability at different temperaturesare presented in Figure 6, and the outcomes from the samples stored at different pH levels are recordedin Figure 7. The effects of time length on stability when the nanoparticles were stored at 25 °C and pH 6.5 for different periods are shown in Figure 8.

The data demonstrates that nanoparticles remained stable at a wide temperature range of 5°C to 45°C (Figure 6a-i). The primary characteristics like particle size and dissolution rate did not change significantly. The dissolution of SM-APSP held at 5°C (Figure 6a) was 48.46%, and when stored at 45°C (Figure 6i), their dissolution was 49.5% in the first 30 minutes of the dissolution test. Unlike those, the nanoparticles that were stored at 25°C had a dissolution rate of 68.2% in the first 30 minutes of the experiment (Figure 6e).

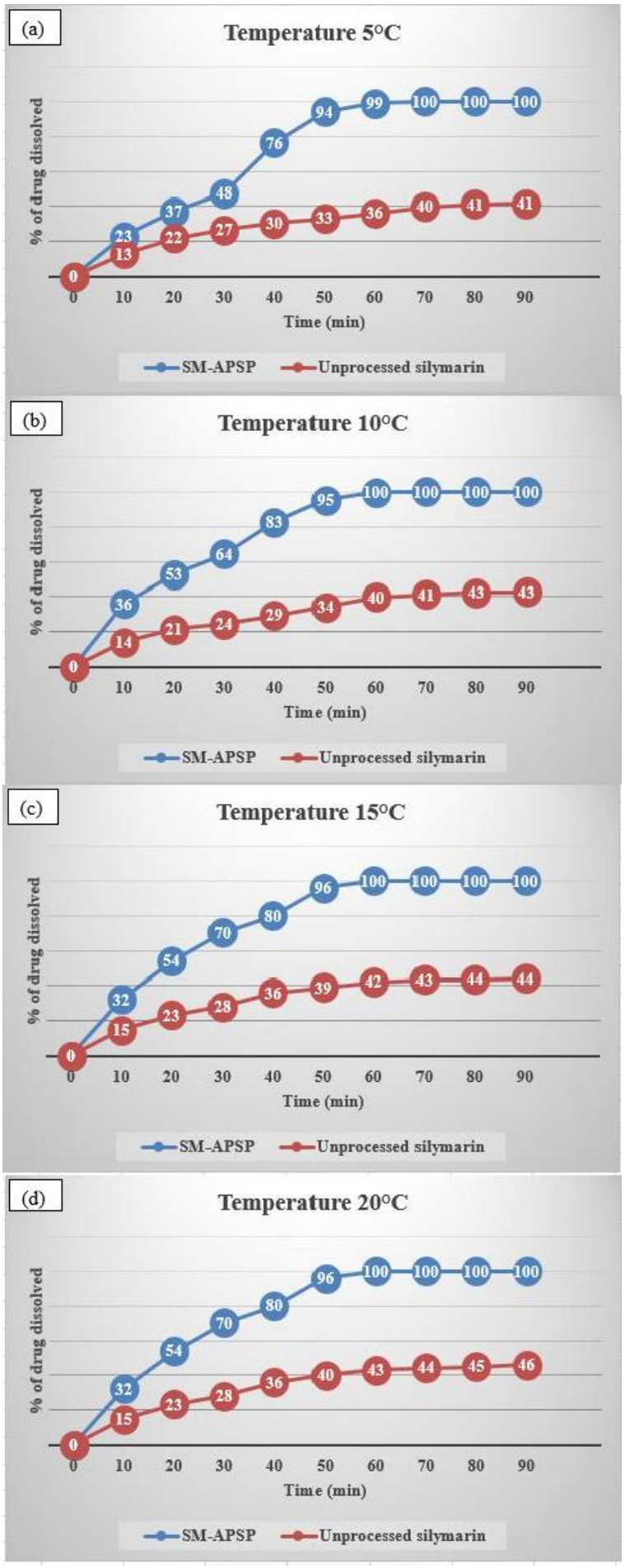
(a)
Temperature 5°C
% of drug dissolved
0 10 20 30 40 50 60 70 80 90
Time (min)
0 23 37 48 76 94 99 100 100 100
0 13 22 27 30 33 36 40 41 41
SM-APSP
Unprocessed silymarin
(b)
Temperature 10°C
% of drug dissolved
0 10 20 30 40 50 60 70 80 90
Time (min)
0 36 53 64 83 95 100 100 100 100
0 14 21 24 29 34 40 41 43 43
SM-APSP
Unprocessed silymarin
(c)
Temperature 15°C
% of drug dissolved
0 10 20 30 40 50 60 70 80 90
Time (min)
0 32 54 70 80 96 100 100 100 100
0 15 23 28 36 39 42 43 44 44
SM-APSP
Unprocessed silymarin
(d)
Temperature 20°C
% of drug dissolved
0 10 20 30 40 50 60 70 80 90
Time (min)
0 32 54 70 80 96 100 100 100 100
0 15 23 28 36 40 43 44 45 46
SM-APSP
Unprocessed silymarin

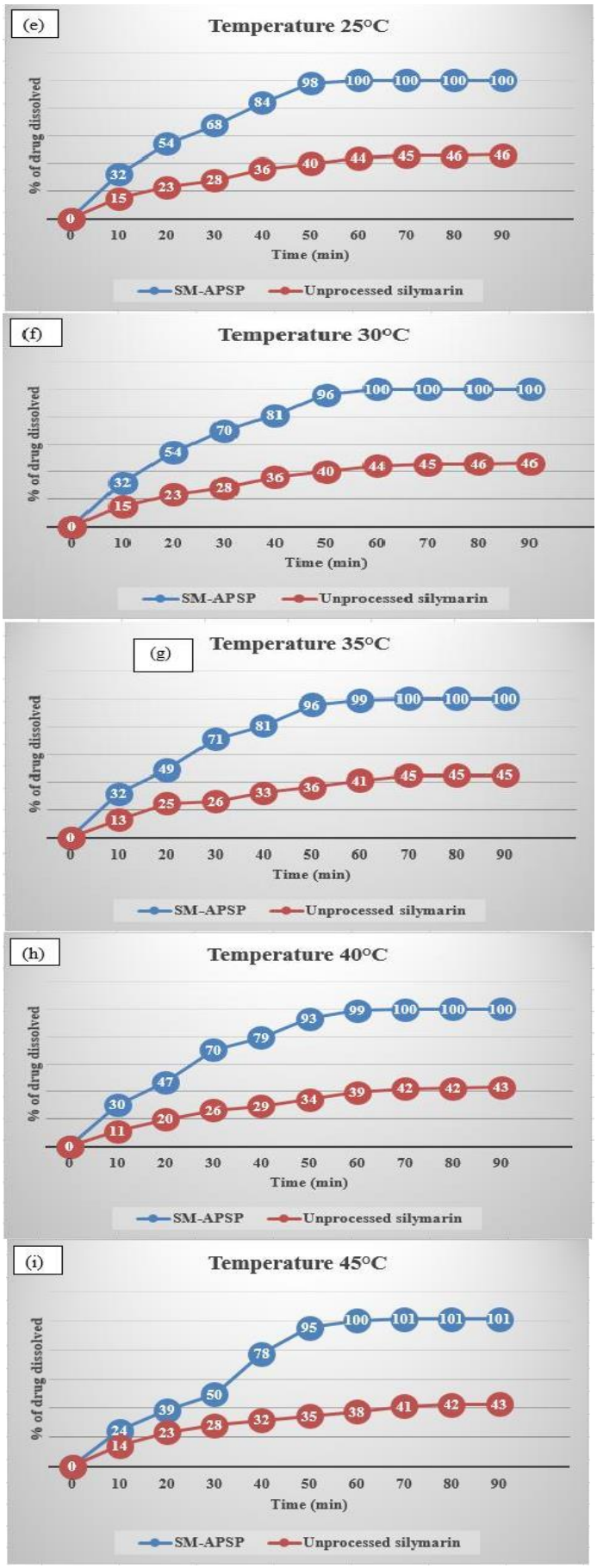

Figure 6. SM-APSP dissolution pattern of SM-APSP after storage at different temperatures

No appreciable modification was noted in the dissolution rates and particle sizes of the nanoform of the drug after storing for 24 weeks except for minor changes in dissolution when stored at the highest and lowest temperature limits. It is already reported that the lots stored at temperatures between 5°C and 30°C demonstrated excellent dissolution profiles [63]. The analysis of the storage stability of the nanoparticles at temperature limits from 5 °C to 30 °C revealed that the data derived from the dissolution of the nanoparticles during long-term storage was not significantly different from each other when compared at different time points. The silymarin content in the lot stored at 25°C and pH 6.5 at the end of the experiment was noted as 98.78%. The products demonstrated desirable stability notwithstanding minor changes in certain cases like a slight lumping effect, observed in samples stored at extreme temperatures. Such samples showed slightly lower rates of dissolution. The optimal temperature range for silymarin nanoparticle storage turns out to be a wide range of 5 to 30°C.

As the pH of a compound during storage, especially if stored for longer periods may also affect its stability [64], therefore, the nanoparticles' stability against pH effects was carefully monitored and the data was collected (Figure 7).

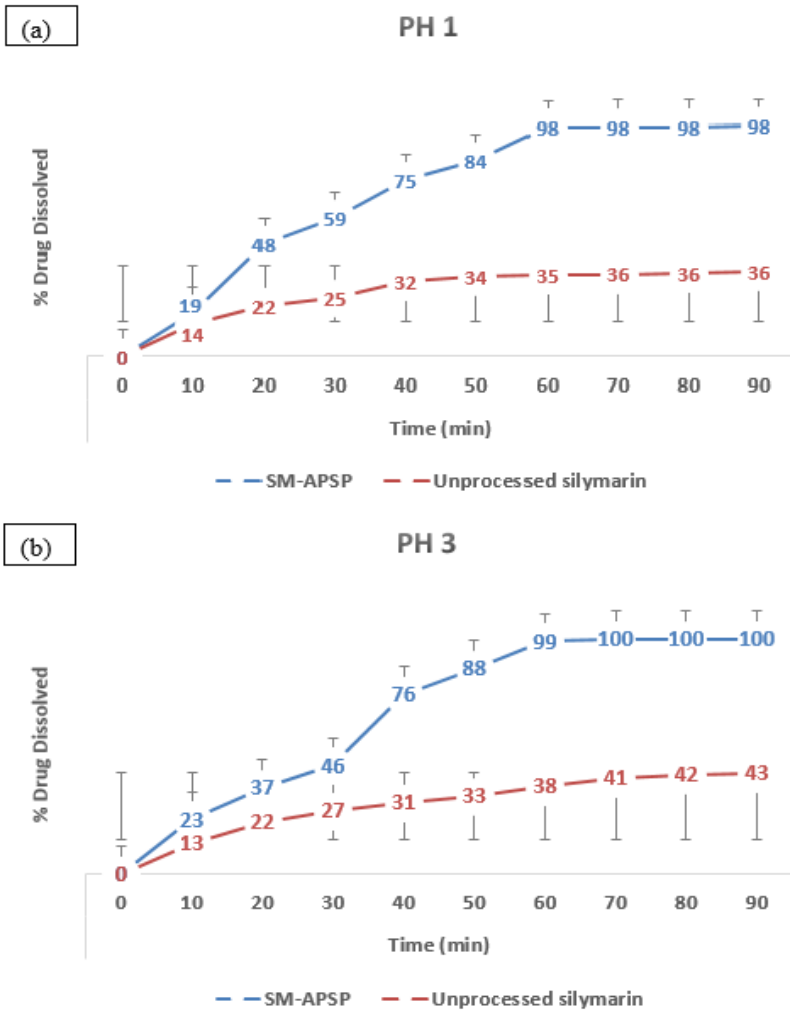

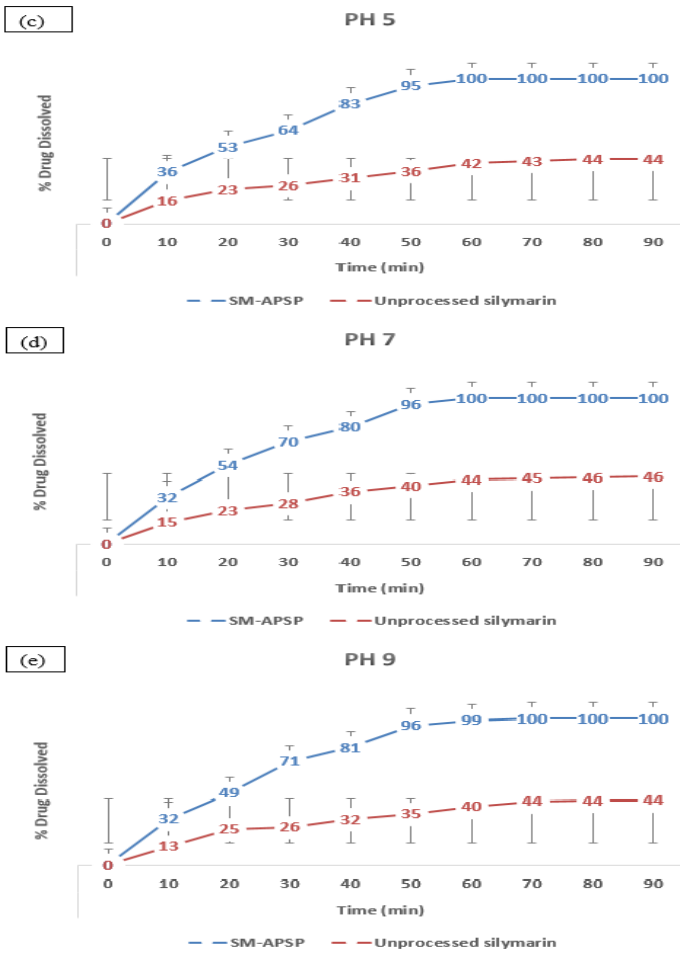

Figure 7. SM-APSP dissolution pattern after storage at pH 1 to 9

Nanoparticles remained stable at a wide pH range and no significant difference was noted in dissolution rate and particle size diameters among them. Especially those stored at pH 5 to 7 (Figures 7c and 7d). The results are suggestive of homogeneous nanoparticles showing desired stability at pH 5 to 7. When the pH moved from 5 to 1 or from 7 onward, the nanoparticles became slightly clumped. As soon as the lumping effects happened at unfavorable conditions, the nanoparticles started to become micrometric and heterogeneous. The dissolution behavior of the nanoparticles also changed, showing slightly slower and incomplete dissolution. It is important to note that pH affects the agglomeration of nanoparticles. On the other hand, the samples held at pH 5 to 7 for up to 24 weeks remained stable. The slow dissolution of nanoparticles and their inability to maintain the initial diameter have also been previously reported for other compounds [65]. Studies with nanoparticles made by usual bottom-up methods have found problems like uncontrolled particle growth [66]. This phenomenon has been observed in suspensions, including nanosuspensions, in which the smaller particles are forced to grow on top of the larger particles, called Ostwald ripening [67]. Therefore, this assessment is crucial because most materials when stored may experience some alterations that may lead to sedimentation, cluster formation, growth of crystals, and even in some cases, chemical reactions may also ensue [68].

Silymarin nanoparticles were also separately stored in suspension form at 25°C and pH 6.5 for up to 180 days. The stored lots were tested for quality parameters at predetermined intervals. They were tested on the day first and after 30, 60, 90, 120, 150 and 180 days. The effects on nanoparticles stability were monitored and the data was recorded (Figure 8a-g). No major changes were noted in the particle sizes and dissolution rates during the analysis.

A temperature range from 5°C to 30°C and pH from 5 to 7 were recorded as the best storage conditions for SM-APSP based on parameters like mean particle size and dissolution rate. When the

nanoparticles were stored at extreme pH and temperature conditions, the data revealed a modest increase in the size of nanoparticles but not beyond 170 nm. The slight change in size over time at extreme temperatures and pH conditions may be due to the agglomeration or merging of nanoparticles with each other [69]. The results show that the nanoparticles can provide a perfect solution to the bioavailability problem posed by poorly water soluble drugs.

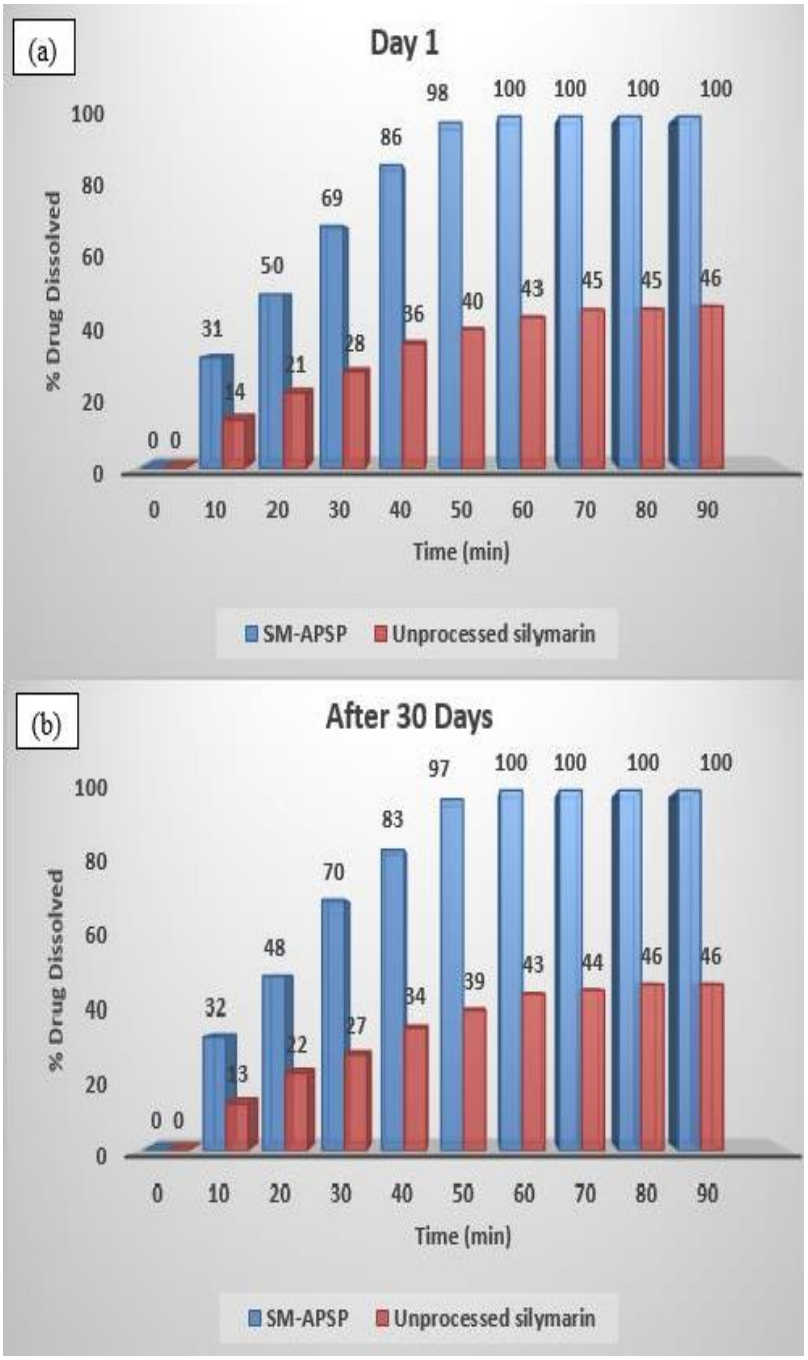

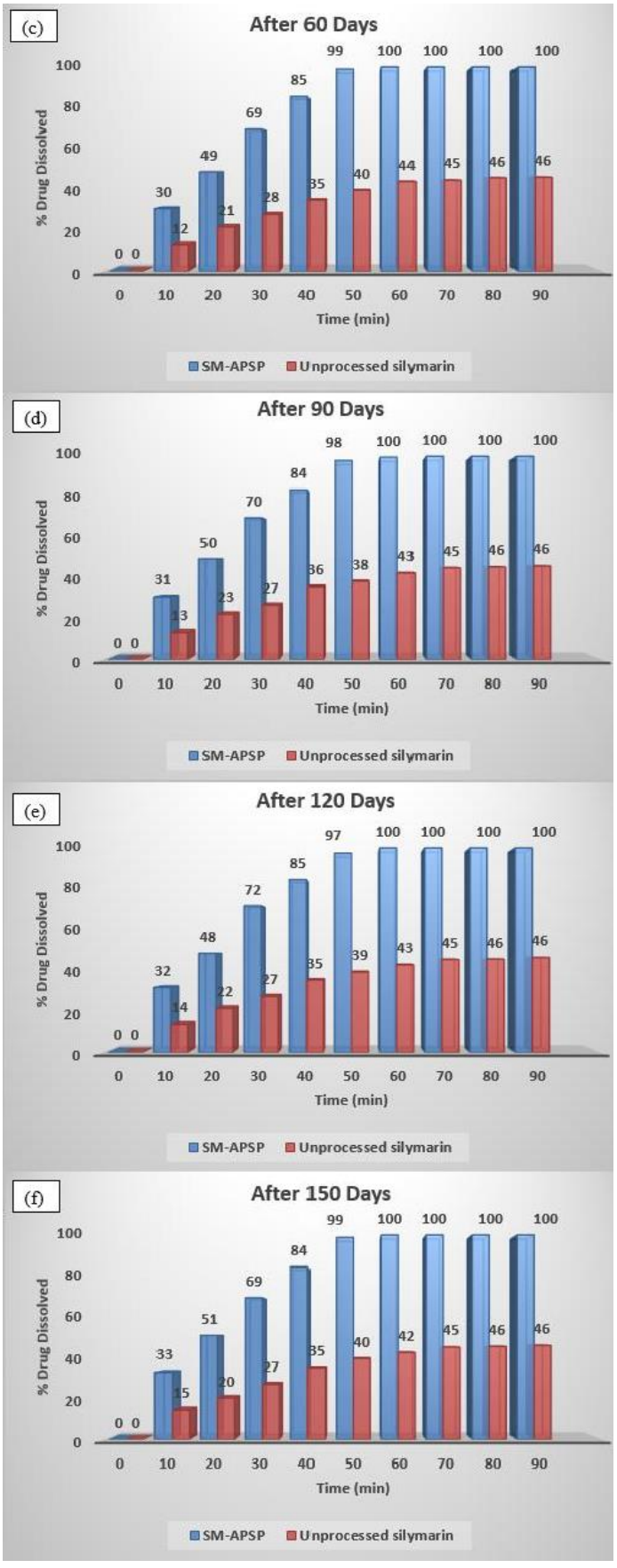
(c)
After 60 Days
% Drug Dissolved
Time (min)
0 0 30 49 69 85 99 100 100 100 100
0 0 12 21 28 35 40 44 45 46 46
SM-APSP
Unprocessed silymarin
(d)
After 90 Days
% Drug Dissolved
Time (min)
0 0 31 50 70 84 98 100 100 100 100
0 0 13 23 27 36 38 43 45 46 46
SM-APSP
Unprocessed silymarin
(e)
After 120 Days
% Drug Dissolved
Time (min)
0 0 32 48 72 85 97 100 100 100 100
0 0 14 22 27 35 39 43 45 46 46
SM-APSP
Unprocessed silymarin
(f)
After 150 Days
% Drug Dissolved
Time (min)
0 0 33 51 69 84 99 100 100 100 100
0 0 15 20 27 35 40 42 45 46 46
SM-APSP
Unprocessed silymarin

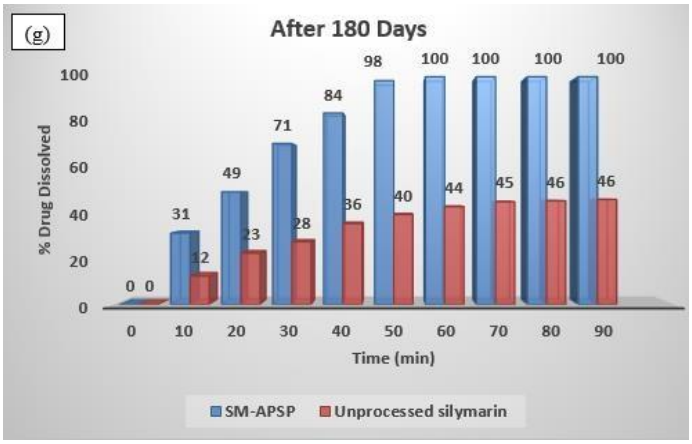

Figure 8. SM-APSP dissolution pattern from first day to 180th day

3.7. Bioavailability study

In this experiment the bioavailability of unprocessed silymarin and the improvement in bioavailability when it was converted to nanoparticle form was determined. Figure 9 shows the readings recorded for respective Tmax, Cmax (µg/mL), AUC (µg-h/mL), and t**1/2** after administration of the samples of unprocessed silymarin and silymarin nanoparticles orally in the same doses to experimental animals. In the case of unprocessed silymarin, the maximum time in hours (T_{max}) to reach maximum plasma concentration (C_{max}) was 0.9 ± 0.36 hours (Figure 9), and it achieved a maximum concentration of 4.48 ± 0.2 (µg/mL). SM-APSP required a time of 0.50 ± 0.11h to acquire a C_{max} of 20.86 ± 0.10 (µg/mL) (Figure 9). If we look at their respective AUCs, the samples, namely unprocessed silymarin and SM-APSP, achieved an AUC of 27.02 ± 1.92 (µg-h/mL) and 279.73 ± 3.54 (µg-h/mL) respectively (Figure 9). The peak plasma concentration (C_{max}) achieved after SM-APSP administration is 4.65 greater, and the area under the curve is 10.352 folds higher than those achieved with the unprocessed silymarin as clear from the data.

The results of comparing the bioavailability of silymarin nanoparticles to unprocessed silymarin show unequivocally that the nanoparticles have significantly improved bioavailability. The results also verified that the rate of dissolution of silymarin had enhanced considerably after conversion to nanometer size, which is in agreement with the previous studies [70]. Particle size reduction results in increased surface free energy, a better wetting of the drug particles, and enhanced surface area, which collectively increase solubility and dissolution rate, which increase bioavailability of drugs. Silymarin conversion to the nanometer range, its transformation into an amorphous state, and its declining crystallinity are the major reasons for enhanced bioavailability [71]. The characterization results also supported this likelihood. Experiments show that converting silymarin to nanoparticle form improved its *in vivo* absorption leading to a higher serum drug concentration, however, the t**1/2** of unprocessed silymarin and SM-APSP do not differ from each other (Figure 9). The results showing a higher bioavailability of SM-APSP than that of the unprocessed silymarin agree with the previous research [45,72].

The above mentioned parameters (T_{max}, C_{max} (µg/mL), AUC (µg-h/mL), and t**1/2**) were calculated forall the test formulations based on serum data. The SM-APSP serum drug titers of the animals were found higher than those of the unprocessed silymarin. The superior bioavailability of SM-APSP than that of the unprocessed silymarin is because the nanoform is better than the unprocessed form in many ways [73]. Due to conversion to the nanoform, the drug's release and absorption were facilitated by its greater surface area and smaller particle size [74]. As silymarin is absorbed more quickly in the nanoparticle form than in the unprocessed form, the enhanced serum level of silymarin nanoparticles administered orally may be the result of particle size reduction [39]. The T_{max} for the nanoparticles is much shorter than the time required for unprocessed silymarin (Figure 9) to reach C_{max}, which is in line with the previous studies [45,75].

The analyses demonstrate undeniably that nanoparticles have many folds higher bioavailability than unprocessed silymarin; therefore, the strategy is successful. The findings suggest that nanoparticles might be a better choice for drug administration because they promote faster solubility and dissolution, which would lead to an effective absorption—the findings that have also been proved earlier [76].

The inadequate bioavailability of poorly water-soluble compounds has been reported by many other authors as well and is linked to the poor absorption rate of the drug [77]. Drugs that are very marginally soluble, mostly have slow rates of dissolution and typically have minimal bioavailability owing to poor *in vivo* absorption [78]. The association of low water solubility with poor oral bioavailability is logical because low aqueous solubility can hamper the bioavailability of unprocessed silymarin. These biopharmaceutical limitations necessitate that silymarin be transformedinto a state that can sufficiently expand its bioavailability because the compound itself has significant clinical efficacy and needs attention. As the drug cannot be made available at the target site in sufficient concentration to exert the required actions, the low bioavailability may result in therapy failure. Therefore, improving a drug's solubility and dissolution right from the beginning can improveits biopharmaceutical features, ensuring optimum therapeutic response [70].

The increased drug surface area, which allowed for better saturation solubility and resulted in a thinner diffusion layer and quicker adherence to the cell membrane, led to a faster absorption of nanoparticles. The smaller the particle size, the greater the cell membrane adhesion, the greater the cell membrane adhesion, the better the saturation solubility which increases the drug saturation inside the cells. Similar reports about nanoparticles have also been put forward before [79]. The smaller particle size also improves membrane permeability allowing more drug molecules to pass through [80].

As advocated above, converting poor water soluble compounds to nanoparticle form appears to be a better strategy for silymarin to increase its oral bioavailability. The ease of preparation of such formulations and minimal requirement for basic ingredients are its standout qualities making them good candidates for industrial production.

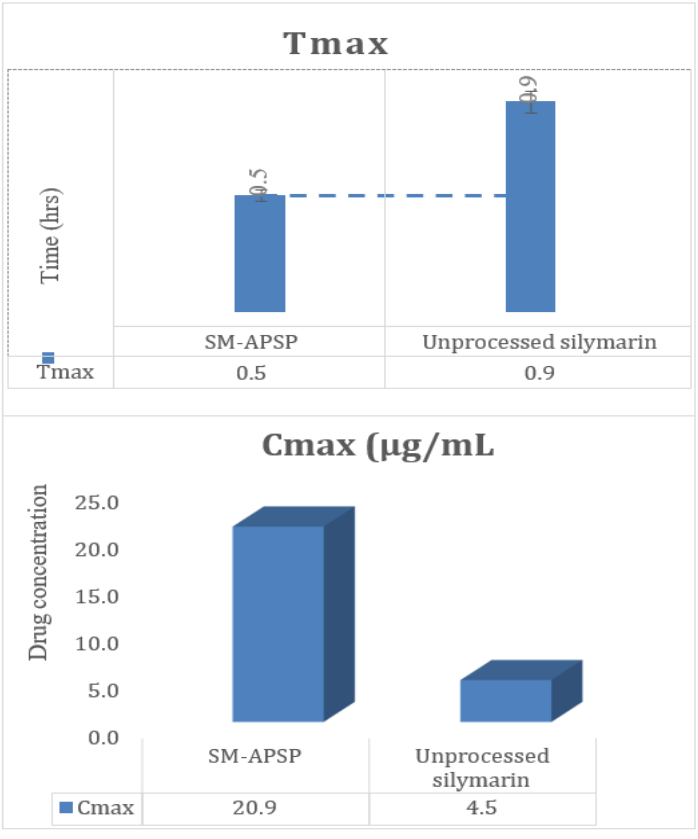

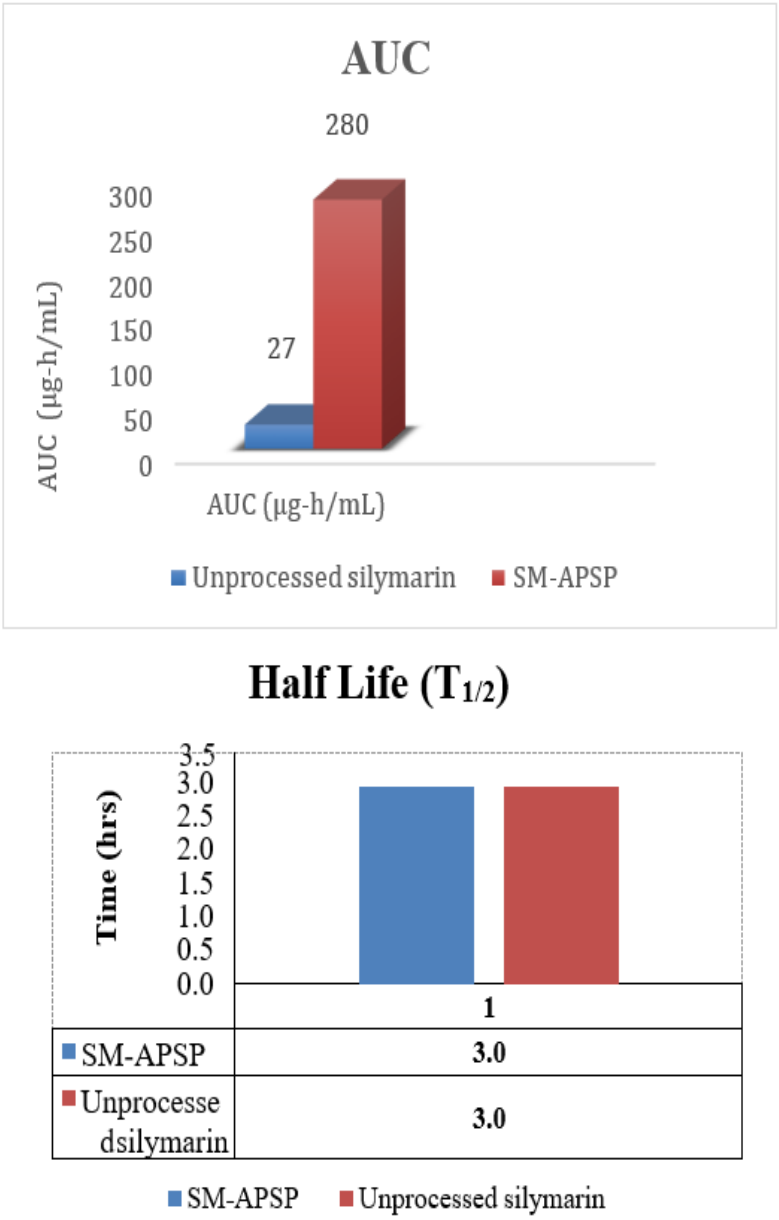

Figure 9. *In vivo* bioavailability study Tmax, [C_{max} (µg/mL)], AUC, and half-life of unprocessed silymarin and SM-APSP

3.8. Hepato-protective activity

In this experiment, SM-APSP efficiency was evaluated to find its hepatoprotective activity against CCl4-induced oxidative stress, liver toxicity, and histological changes in the liver. As acute hepatotoxicity was caused by administering CCl4 to experimental rats, the data from group 2 animals confirm that the dosage is appropriate and sufficient to induce hepatic injury (Table 4). This is evident from the high level of serum marker enzymes and decreased total proteins and albumin values along with the histopathological changes of hepatic tissue (Tables 4, 5, and Figure 10). Increased levels of marker enzymes in serum prove that the hepatocellular membrane's structural integrity has been compromised due to CCl4 toxicity, allowing these enzymes to leak into the blood.

Table 4. Effects of unprocessed silymarin and SM-APSP on LFTs value

S. No	Animal groups	After two weeks			After four weeks			After six weeks		
		ALP (IU/L)	ALT (IU/L)	AST (IU/L)	ALP (IU/L)	ALT (IU/L)	AST (IU/L)	ALP (IU/L)	ALT (IU/L)	AST (IU/L)
1	Untreated group(Positive Control)	71.080 ± 1.20	54.600 ± 0.94	63.66 ± 1.70	70.90 ± 0.030	54.850 ± 0.6	64. 04 ± 1.1	71.100 ± 0.2	55 ± 0.94	63.75 ± 1.2
2	CCl4 TreatedControl (Negative Control)	144.67 ± 1.11	140.13 ± 2.17	104.21 ± 2.40	151.34 ± 1.23	155.26 ± 1.6	110.13 ± 1.10	177.18 ± 1.56	167.13 ± 2.25	119.88 ± 2.15
3	Unprocessed Silymarin 200 mg/kg	134.89 ± 1.22	101.33 ± 1.11	94.290 ± 1.12	114.78 ± 01.1	80.26 ± 1.47	81.74 ± 1.12	99.73 ± 1.64	65.91 ± 1.25	66.29 ± 0.33
4	SM.APSP-75 mg/kg	134.13 ± 0.56	100.06 ± 1.43	92.010 ± 1.33	114.0 ± 1.55	78.17 ± 1.36	80.21 ± 0.41	98.65 ± 0.21	65.17 ± 0.8	64.30 ± 0.23
5	SM.APSP-50 mg/kg	140.12 ± 1.39	119.91 ± 1.83	99.840 ± 2.17	134.51 ± 1.47	100.13 ± 2.78	89.110 ± 1.8	115.92 ± 1.3	85.78 ± 1.54	75.94 ± 1.40

Effect of Silymarin Particle Size on its Solubility and Oral Bioavailability, the Enhancement of Pharmacological Actions

Table 5. Effect of unprocessed silymarin and SM-APSP on total protein and albumin level in serum

S.No	Animal groups	After two weeks		After four weeks		After six weeks	
		Total proteins (IU/L)	Albumin (g/dl)	Total proteins (IU/L)	Albumin (g/dl)	Total proteins (IU/L)	Albumin (g/dl)
1	Untreated group (Positive Control)	6.92 ± 0.97	2.89 ± 0.30	6.88 ± 0.88	2.93 ± 0.101	6.91 ± 1.06	2.90 ± 0.061
2	CCl4 Treated Control (Negative Control)	4.93 ±0.20	2.41 ± 0.20	4.37 ± 1.03	2.18 ± 0.01	4.18 ± 1.07	1.47 ± 0.052
3	Unprocessed Silymarin 200 mg/kg	5.79 ± 0.63	2.58 ± 0.05	5.89 ± 0.76	2.65 ± 0.10	6.40 ± 1.58	2.73 ± 0.03
4	SM.APSP-75 mg/kg	5.84 ± 0.18	2.61 ± 0.30	5.97 ± 1.24	2.70 ± 0.02	6.48 ± 1.13	2.79 ± 0.04
5	SM.APSP-50 mg/kg	5.20 ± 0.66	2.56 ± 0.20	5.50 ± 1.22	2.66 ± 0.06	6.02 ± 1.08	2.69 ± 0.046

3.8.1. Effect of unprocessed silymarin and SM-APSP on CCl4-induced changes in plasma AST, ALT, and ALP

A significant increase in the levels of ALP, ALT, and AST was noted in the sixth week in the plasma of animals intoxicated with CCl4 (ALP 177.18 ± 1.56, ALT 167.13 ± 2.25, AST 119.88 ± 2.150) in contrast to the standard control group (ALP 71.100 ± 0.20, ALT 55.0 ± 0.940, AST 63.750 ± 1.20) (Table 4). However, when the rats were treated with different silymarin samples, a noticeable recovery was seen in these parameters. Compared with the group intoxicated with CCl4 and not receiving silymarin, the rats treated with unprocessed silymarin 200mg/kg b.w, SM-APSP-75, and SM-APSP-50 showed a minimal change in the values of biochemical parameters (Table 4). Treatmentwith 200 mg/kg of unprocessed silymarin and SM-APSP at doses of 50 and 75mg all showed hepatoprotective activity; however, unprocessed silymarin (200mg/kg) and SM-APSP-75 (75mg/kg) showed significant protective actions, and both drugs seemed almost equally ameliorative. An amelioration seen in the levels of ALP, ALT, and AST after the administration of unprocessed silymarin 200mg/kg and SM-APSP-75, warrant the drug's hepatoprotective actions (Group 3-4). Afterusing SM-APSP-75, the liver protection effect was at its maximum, as evident from the values of serum marker enzymes observed in Group 4 animals at 6^{th}.week (Table 4). The values are a demonstration of the magnitude of the hepatoprotection these drugs offered. Rats treated with SM- APSP-75 recorded a clear reduction in ALT, AST, and ALP levels compared to all other groups, suggesting an enhanced hepatoprotection with nanoparticles at this dose.

3.8.2. Effect of silymarin and SM-APSP on CCl4 induced change in total protein and albumin levels

Markedly decreased levels of total proteins and albumin were noted in the tested animals in the sixth week intoxicated with CCl4 (TP 4.18 ± 1.07 IU/L and albumin 1.47 ± 0.052 g/dl) in contrast to the standard control group (TP 6.91 ± 1.06 IU/L and albumin 2.90 ± 0.061 g/dl) as shown in Table 5.

However, a recovery towards normal was observed in the levels of total proteins and albumin when the rats were treated with unprocessed silymarin 200mg/kg, SM-APSP-75, and SM-APSP-50 (Table 5). A minimal negative change in the values of total proteins and albumin was seen in the group receiving SM-APSP-75 and silymarin 200mg/kg (Table 5). Generally, treatments with all silymarin samples showed hepatoprotective activity; however, SM-APSP-75 (75mg/kg) showed significant and maximum protective action. When unprocessed silymarin and SM-APSP were administered (Groups 3–5), an amelioration was seen in the levels of total proteins and albumin, showing that the drugs are extending hepatoprotection. However, the data also shows that when silymarin nanoparticles were used at 75mg/kg dose, ((Table 5, group 4), there was a notable amelioration in the levels of these parameters. At this dose, the liver protection effect was at its maximum (Table 5). Rats treated with SM-APSP-75 revealed a notably increased level of total proteins and albumin, suggesting enhanced hepatoprotection with nanoparticles. In summary, after treatment with carbon tetrachloride, the levels of ALP, ALT, and AST were significantly increased and total proteins and albumin values were decreased over time in experimental rats. After treatment with SM-APSP-75, these values were recovered to normal.

As silymarin is a well-known Hepatoprotective agent, we can see that total proteins and albumin levels across all treated groups increased when they received unprocessed silymarin, SM-APSP-75, or SM-APSP-50 (groups 3, 4, and 5), but the enhancement in the levels remained different dependingon the sample received and its dose. The best hepatoprotective result was obtained by using SM- APSP-75, which recorded a notable recovery, therefore, we can call it the best drug out of the pool we tested.

3.8.3. Time-Dependent effects of silymarin and SM-APSP

The results of time-dependent effects of silymarin and SM-APSP on ALP, ALT, AST, total proteins, and albumin levels were also recorded and prominent differences in the effects of the samples on these markers were noted depending on the duration for which the drugs were administered (Tables 4 and 5). Data was collected depending on time, i.e., after treating the animals for 2, 4, and 6 weeks,to find the optimum time point (from 2 to 6 weeks) at which the samples showed the best results in terms of hepatoprotective effects. As the data was collected in the second, fourth, and sixth weeks, there was a continuous declining trend in the ALP, ALT, and AST values (Table 4) and an increasingtrend in the levels of total proteins and albumin in the animals receiving treatment (Table 5).

Results correlate the healing effects on serum enzymes to the length of treatment duration. It is pertinent to mention that at every stage of monitoring its effects, SM-APSP-75 showed the best effects compared to other samples. When used for 6 weeks, SM-APSP-75 significantly reduced the values of the serum marker enzymes compared to the results when the samples were used for two or four weeks. Total Proteins and albumin recovery toward normal values for time duration showed the samebehavior, and the maximum recovery was recorded in the sixth week of the experimental period (Table 5). The group receiving the dose of 50 mg/kg b.w. also brought about desired changes in the selected parameters, however, those were comparatively less in magnitude (Tables 4 and 5).

Results demonstrate that compared to the group receiving only CCl_4 treatment, the groups receiving treatment with CCl_4 plus SM-APSP or silymarin enjoyed considerable liver protection. They showed lower ALP, ALT, and AST values and higher total proteins, and albumin levels in a fashion depending on dose received and treatment time duration. In the same way, dissimilar to the control group, CCl_4 exposure increased the ALP, ALT, and AST concentrations in the groups and decreased total proteins and albumin levels. SM-APSP-75 exhibited the best hepatoprotective effects.

3.8.4. Effect of unprocessed silymarin and SM-APSP on hepatic histopathology

Each group's hematoxylin and eosin-stained liver tissue slices were examined to measure histological changes in the liver. Healthy, untreated livers did not show pathological alterations. The animals from that group displayed the normal, healthy lobular architecture of liver tissue, including a central vein and radiating hepatic cords [Figure 10 (1)].

On the contrary, on macroscopic examination, the CCl_4-treated rats' livers showed severe

hepatocellular damage, they were larger, paler, and had uneven surfaces. Rats in this group had lost normal hepatic structure. Carbon tetrachloride had caused centrilobular necrosis and degeneration.

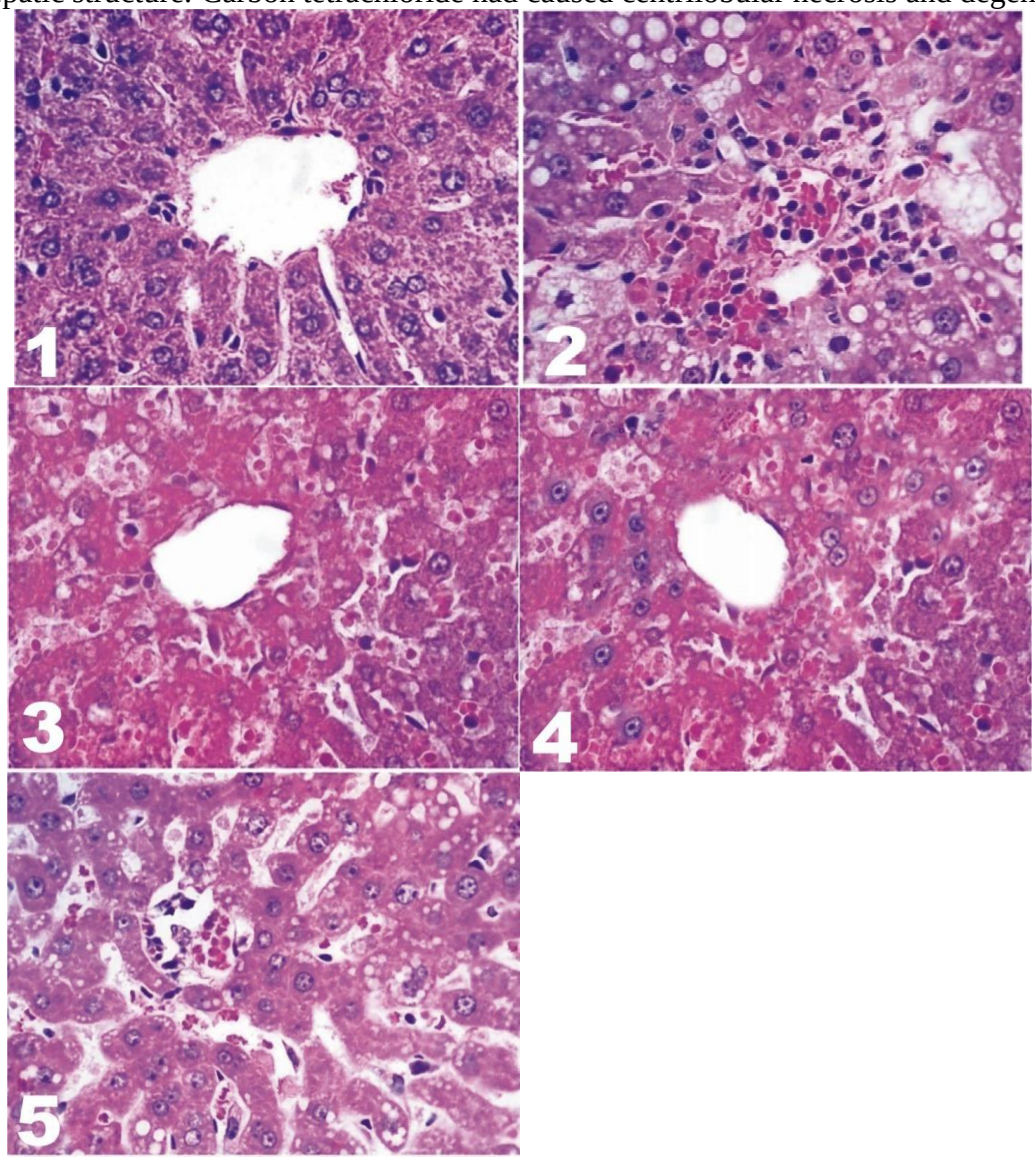

[Figure 10 (1) Hepatic histology of untreated control (normal round-shaped central veins, plates of hepatocytes, and sinusoidal spaces), 2) Hepatic histology of CCl4 treated control (central veins congestion, macro and microvesicular steatosis, and hepatocytes with necrosis). Notable histopathological changes in liver histoarchitecture, 3) Effect of unprocessed silymarin (200mg/kg. b.w.) on hepatic histology of CCl4 treated rats after six weeks (congested central veins, macrovesicular, and necrotic hepatocytes. Some minor changes in histology and normal liver histoarchitecture (micro vesicular steatosis), 4) Effect of SM.APSP-75mg on hepatic histology of CCl4 treated rats after six weeks (micro vesicular steatosis), and 5)] Effect of SM.APSP-50mg on hepatic histology of CCl4 treated rats after six weeks (sinusoidal dilatation and micro vesicular steatosis).

Severe liver injury following CCl4 exposure was characterized by the rupture, disarray, and deformability of the hepatocytes; the lattice nature of the hepatocytes was disrupted [Figure 10 (2)]. Acute liver damage caused by CCl4 was clear from the damage to the membrane of cells, reduced diameters of nuclei, disintegration of the central vein, dilated sinusoids, and a modest infiltration of monocytes and neutrophils into the cytoplasm. Extensive hepatocyte necrosis grew more noticeable in centrizonal areas (zone 3 necrosis). There was hepatocyte proliferation, cells with a small number of mitotic configurations, scattered Kupffer cells, the portal, and central veins became congested, a

ballooning degeneration of parenchymal cells of the liver, and fatty vacuolation throughout the liver relative to the other animals group not exposed to CCl_4. Additionally, as a result of the acute liver damage brought on by CCl_4, the nuclear membrane had shrunk and destroyed, and there were numerous vesicles visible in the cytoplasm. However, the pathological changes that took place in groups treated with SM-APSP were not as severe because these changes got reversed with treatment. The reversal of CCl_4 caused damage depending upon the dose and type of sample used are presented in Figure 10 (3-5).

Drugs such as CCl_4 and paracetamol, may also cause hepatic injury, the reason of about two million deaths per year [12]. The transformation of CCl_4 into CCl_3 radicals in mammalian hepatic parenchyma cells by cytochrome P450 is thought to be the basis of CCl_4 hepatotoxicity. The animal model of hepatic damage induced by CCl_4 shares some characteristics with various types of human hepatic cirrhosis in terms of biochemical elements and morphological implications of collagen metabolic activities. Therefore, we preferred to use CCl_4 to induce hepatic injury experimentally in rats.

Silymarin is an excellent antioxidant, free radicals scavenger, and anti-fibrotic agent; the effects that together contribute to its hepatoprotective activity and is used globally for this purpose. However, these vital benefits are reduced by the poor aqueous solubility of silymarin (<50 μg/mL) and poor intestinal absorption. Because of that attempts are made to enhance its oral absorption to increase the bioavailability of this exceptional biomolecule [81]. The markers (ALP, ALT, and AST) generally regarded as reliable indicators of hepatocellular injury, showed increased presence in serum after CCl_4 exposure, denoting liver damage. The animal groups were treated with SM-APSP-50, SM-APSP-75, and unprocessed silymarin, each showing a depression in the marker enzyme levels depending on the type of silymarin sample used.

The SM-APSP-75 offered the best effects which may be possible due to the presence of SM-APSP in hepatocytes in the maximum possible concentration, relative to the dose used [82]. A greater concentration of SM-APSP must have resulted from a better absorption of SM-APSP into the hepatocytes and a better silymarin absorption was made possible due to better solubility and dissolution properties of silymarin nanoparticles [83], which is the purpose of this experiment.

The results point towards the improvement in silymarin performance in nanoparticle form in comparison to unprocessed silymarin. Unprocessed silymarin showed a degree of hepatoprotection at 200 mg/kg dosage, which is even lesser than the effects shown by SM-APSP at 75mg/kg b.w. dose. Our findings are the first of their kind to demonstrate that SM nanoparticles possess significant hepatoprotective effects at a dose of 75mg/kg b.w. However, other reports exist where nanoparticles prepared by other methods, showed enhanced hepatoprotection [84]. According to El-Nahas AE et al. 2017, their nanoparticles showed superior effects compared to the effects shown by commercial silymarin in rats exposed to CCl_4. In another report, scientists prepared silymarin-loaded lipid polymer hybrid nanoparticles that had superior oral delivery and achieved better effects on lowering lipids in mouse models. They reported many fold increase in oral bioavailability of silymarin [83]. Similarly, Nasr SS et al. 2019 who synthesized silymarin-loaded mesoporous silica nanoparticles, reported that when orally used they are significantly superior to unprocessed silymarin [85]. Kumar et al. designed a study to increase silymarin oral bioavailability and achieved very encouraging results [86]. There are various other examples where the oral bioavailability of less water soluble drugs was improved after converting them from an unprocessed form to nanoform [77,79,81]. The dissimilarities noted in ALP, ALT, AST, TP, and albumin levels across the groups caused by better effects of SM-APSP after the same treatment duration at a lower dose in our study can be explained by SM-APSP particle size, which is the only difference among the samples. SM-APSP has a particle size in the nanometer range, which results in better solubility and absorption while unprocessed silymarin cannot do that because of larger particle sizes. A better absorption ensures silymarin presence in higher concentrations on the required target site to produce more effects and can better reverse the disturbed hepatic antioxidant status. The resulting larger surface area of particles ensures better wetting, which is responsible for better solubility and absorption [87]. This may explain why the effects of SM-APSP

at 75mg/kg b.w., are better than those of unprocessed silymarin at 200mg/kg b.w. dose. The explanation is understandable because better absorption of drugs leads to higher concentrations at the target site, where they are needed for action [88].

CCl_4 also caused histopathological abnormalities in the livers of rats [89] the magnitudes of which was which was different in each group because each group received different treatment. The findings of this study support using SM-APSP because it healed the histopathological abnormalities and necroinflammatory lesions in a superior way. Previous works by researchers have also demonstrated the potential of silymarin to alter CCl_4 induced histopathological modifications like ballooning and necrosis [90,91], which match our results. However, the results from this study also proved the far better effects of silymarin nanoparticles. This difference in the levels of affectivity is attributed to better absorption because of small-sized particles and larger surface areas of SM-APSP [87]. If more quantities of silymarin are absorbed, it will be present in more concentration on the required target site to produce more effects and will reverse the disturbed hepatic antioxidant status.

Furthermore, reduced fatty infiltration, mild portal inflammation, and the extent of necrosis in the liver were signs of partial hepatic protection following treatment with a low SM-APSP dose(50mg/kg) as shown in Figure 10 (5). Treatment using a higher dose [SM-APSP (75mg/kg)]significantly ameliorated these alterations Figure 10 (4). At a dose of 75mg SM-APSP/kg b.w., verylow levels of inflammatory cell infiltration and necrotic liver cells were noticed. These tests established a promising and far better hepatoprotective role of SM-APSP, because they have better absorption and may prove a good alternative to the unprocessed silymarin. SM-APSP-75 enabled anenormous decrease of over 100% in the required silymarin dose and at the same time offered better therapeutic outcomes. In this way, SM-APSP can save our raw material sources and can also save thesubjects from unnecessary drug burden and its side effects.

The study demonstrated that CCl_4 induced oxidative stress in rats' liver yielded to SM-APSP because of the better antioxidant property of the latter that is also previously reported by other researchers, although, they synthesized nanoparticles using other methods [92,93]. The protective action further improved by increasing the dose from 50 to 75mg/kg b.w., which is an expected behavior of drugs. This may be recommended that the drug SM-APSP in high doses (75mg/kg b.w) may confer the best hepatoprotective effects with a notable improvement in the hepatic histopathological picture. Our findings support that SM-APSP can protect liver better than unprocessed silymarin and improve its histological profile. Along with antilipid peroxidative and antioxidant activities, nanoparticles may have fully restored the liver enzyme system unlike unprocessed silymarin and aided in liver regeneration [23].

Rapid turnaround of total proteins and albumin levels by SM-APSP and down regulation of serum enzyme parameters all made possible by the conversion silymarin to nanoparticles, which improved silymarin solubilization. The enhanced pharmacological effects were achieved because of a better dissolution rate of the drug in the nanoparticle form. The solubility and oral bioavailability of silymarin improved by using nanotechnology. The prepared nanoparticles could be formulated as future drugs for use in treating human liver diseases and other morbid conditions. The integration of phytotherapy and nanotechnology at the clinical level will boost pharmacological response and favorable clinical results for the ailing population [29]

4. Conclusion

According to the present study, between APSP and EPN methods, APSP is the best method for the synthesis of silymarin nanoparticles. This is demonstrated by the characterization findings and, subsequently, by the silymarin nanoparticles' improved pharmacological effects. The solubility and dissolution of the prepared nanoparticles were manyfold increased compared to their respective unprocessed drugs. In comparison to silymarin that had not been processed, the nanoparticles' hepatoprotective properties in terms of how they affected liver enzymes and histology were also significantly boosted. Silymarin nanoparticles made using the APSP approach are recommended for clinical research in light of the aforementioned information.

References

1. Bayda S, Adeel M, Tuccinardi T, Cordani M, Rizzolio F. The history of nanoscience and nanotechnology: from chemical–physical applications to nanomedicine. Molecules, 25 (1), 112 (2019).
2. Bayón-Cordero L, Alkorta I, Arana L. Application of solid lipid nanoparticles to improve the efficiency of anticancer drugs. Nanomaterials, 9(3):474, (2019).
3. Afarid M, Mahmoodi S, Baghban R. Recent achievements in nano-based technologies for ocular disease diagnosis and treatment, review and update. Journal of Nanobiotechnology, 20(1):1- 36, (2022).
4. Ali J, Hussain A, Rehman S, Khan FA, Sher M. Antifungal potential of Mentha piperita leavesand stem extracts against phytopathogenic fungi. Specialty Journal of Biological Sciences, 3, 38-43 (2017).
5. Newman DJ, Cragg GM. Natural products as sources of new drugs over the nearly four decades from 01/1981 to 09/2019. Journal of natural products. 2020 Mar 12;83(3):770-803.
6. Zaman MA, Abbas RZ, Qamar W, Qamar MF, Mehreen U, Shahid Z, Kamran M. Role of secondary metabolites of medicinal plants against Ascaridia galli. World's Poultry Science Journal. 2020 Jul 2; 76 (3):639-55.
7. Cosme P, Rodríguez AB, Espino J, Garrido M. Plant phenolics: Bioavailability as a key determinant of their potential health-promoting applications. Antioxidants, 9(12), 1263 (2020).
8. Gheorghita, G.R.; Paun, V.I.; Neagu, S.; Maria, G.-M.; Enache, M.; Purcarea, C.; Parvulescu, V.I.; Tudorache, M. Cold-Active Lipase-Based Biocatalysts for Silymarin Valorization through Biocatalytic Acylation of Silybin. Catalysts, 11(11), 1390 (2021).
9. Bhattacharya, S. "Nuts and Seeds in Health and Disease Prevention" 2nd ed.; West Bengal Medical Services Corporation Ltd.: Kolkata, India, pp. 429–438 (2020).
10. Shapovalova V. Alcoholic Hepatitis: An experimental meta-analysis. SSP Modern Pharmacy and Medicine. 2023 Feb 16;3(1):1-1.
11. Camini FC, Costa DC. Silymarin: Not just another antioxidant. Journal of basic and clinical physiology and pharmacology, 31(4), 20190206 (2020).
12. Shakya AK. Drug-induced hepatotoxicity and hepatoprotective medicinal plants: a review. Indian Journal of Pharmaceutical Education and Research, 54(2), 234-50 (2020).
13. Marmouzi I, Bouyahya A, Ezzat SM, El Jemli M, Kharbach M. The food plant *Silybum marianum* (L.) Gaertn.: Phytochemistry, Ethnopharmacology, and clinical evidence. Journal of Ethnopharmacology, 265, 113303-113303 (2021).
14. Adetuyi BO, Omolabi FK, Olajide PA, Oloke JK. Pharmacological, biochemical and therapeutic potential of milk thistle (silymarin): a review. World News of Natural Sciences, 37(2021),75-91 (2021).
15. Giustarini D, Milzani A, Dalle-Donne I, Rossi R. How to Increase Cellular Glutathione. Antioxidants, 12(5), 1-20 (2023).
16. Samee A, Amir RM, Ahmad A, Watto FM, Ali M, Azam MT, Sheeraz M, Fatima H, Zahoor Z, Zahid M, Ashraf H. Effectiveness of Milk Thistle on Human Body against Diseases: A Comprehensive Review. Scholars Bulletin, 9(2), 8-18 (2023).
17. Assis-Júnior EM, Melo AT, Pereira VB, Wong DV, Sousa NR, Oliveira CM, Malveira LR, Moreira LS, Souza MH, Almeida PR, Lima-Júnior RC. Dual effect of silymarin on experimental non-alcoholic steatohepatitis induced by irinotecan. Toxicology and Applied Pharmacology, 327(2017), 71-9 (2017).
18. Mangwani N, Singh PK, Kumar V. Medicinal plants: adjunct treatment to tuberculosis chemotherapy to prevent hepatic damage. Journal of Ayurveda and Integrative Medicine, 11(4), 522-28 (2020).
19. Kheong CW, Mustapha NR, Mahadeva S. A randomized trial of silymarin for the treatment of nonalcoholic steatohepatitis. Clinical Gastroenterology and Hepatology. 2017 Dec 1;15(12):1940-9.

20. Colletta C, Colletta A, Placentino G. Lifestyle and silymarin: a fight against liver damage in NAFLD associated-prediabetic disease. Journal of Diabetes & Metabolic Disorders, 19(2020), 883- 94 (2020).
21. Curcio A, Romano A, Cuozzo S, Di Nicola A, Grassi O, Schiaroli D, Nocera GF, Pironti M. Silymarin in combination with vitamin C, vitamin E, coenzyme Q10 and selenomethionine to improveliver enzymes and blood lipid profile in NAFLD patients. Medicina, 56(10), 544 (2020).
22. Beydilli H, Yilmaz N, Cetin ES, Topal Y, Celik OI, Sahin C, Topal H, Cigerci IH, Sozen H. Evaluation of the protective effect of silibinin against diazinon induced hepatotoxicity and free-radical damage in rat liver. Iranian Red Crescent Medical Journal, 17(4), e25310 (2015).
23. Shriram RG, Moin A, Alotaibi HF, Khafagy ES, Al Saqr A, Abu Lila AS, Charyulu RN. Phytosomes as a plausible nano-delivery system for enhanced oral bioavailability and improved hepatoprotective activity of silymarin. Pharmaceuticals, 15(7), 790-809 (2022).
24. El-Far M, Salah N, Essam A, Abd El-Azim AO, El-Sherbiny IM. Silymarin nanoformulation as a potential anticancer agent in experimental Ehrlich ascites carcinoma-bearing animals. Nanomedicine, 13(15), 1865-58 (2018).
25. Anushiravani A, Haddadi N, Pourfarmanbar M, Mohammadkarimi V. Treatment options for nonalcoholic fatty liver disease: a double-blinded randomized placebo-controlled trial. European journal of gastroenterology & hepatology, 31(5), 613-7 (2019).
26. Wang X, Zhang Z, Wu SC. Health benefits of *Silybum marianum*: Phytochemistry, pharmacology, and applications. Journal of agricultural and food chemistry, 68(42), 11644-64 (2020).
27. Zhu HJ, Brinda BJ, Chavin KD, Bernstein HJ, Patrick KS, Markowitz JS. An assessment of pharmacokinetics and antioxidant activity of free silymarin flavonolignans in healthy volunteers: a dose escalation study. Drug Metabolism and Disposition. 2013 Sep 1;41(9):1679-85.
28. Hosseini S, Rezaei S, Moghaddam MR, Elyasi S, Karimi G. Evaluation of oral nano-silymarin formulation efficacy on prevention of radiotherapy-induced mucositis: A randomized, double-blinded, placebo-controlled clinical trial. PharmaNutrition, 15(2021), 100253 (2021).
29. Sher M, Zahoor M, Shah SW, Khan FA. Is particle size reduction linked to drug efficacy: an overview into nano initiatives in Pharmaceuticals. Zeitschrift für Physikalische Chemie. 2023 Jun 2(0).
30. Khan FA, Zahoor M, Islam NU, Hameed R. Synthesis of Cefixime and Azithromycin Nanoparticles. Journal of Nanomaterials, 2016, 29-37 (2016).
31. Mohamed MS, Abdelhafez WA, Zayed G, Samy AM. Optimization, in-vitro release, and in- vivo evaluation of gliquidone nanoparticles. AAPS PharmSciTech, 21(2), 1-2 (2020).
32. Kakran M, Sahoo NG, Tan IL, Li L. Preparation of nanoparticles of poorly water-soluble antioxidant curcumin by antisolvent precipitation methods. Journal of Nanoparticle Research. 14(2012), 1-11 (2012).
33. Kakran M, Sahoo NG, Li L, Judeh Z. Fabrication of quercetin nanoparticles by anti-solvent precipitation method for enhanced dissolution. Powder Technology, 223(2012), 59-64 (2012).
34. Campodónico A, Collado E, Ricci R, Pappa H, Segall A, Pizzorno MT. Dissolution test for silymarin tablets and capsules. Drug development and industrial pharmacy, 27(3), 261-5 (2001).
35. Sharma S, Jaiswal S, Duffy B, Jaiswal AK. Nanostructured materials for food applications: spectroscopy, microscopy, and physical properties. Bioengineering, 6(1), 26-42 (2019).
36. Racault C, Langlais F, Naslain R. Solid-state synthesis and characterization of the ternary phaseTi 3 SiC 2. Journal of Materials Science, 29(13), 3384-92 (2004).
37. Siekmann B, Westesen K. Thermoanalysis of the recrystallization process of melt- homogenized glyceride nanoparticles. Colloids and surfaces B: Biointerfaces, 3(3):159-75 (2004).
38. Khan BA, Rashid F, Khan MK, Alqahtani SS, Sultan MH, Almoshari Y. Fabrication of capsaicin loaded nanocrystals: Physical characterizations and in vivo evaluation. Pharmaceutics, 13(6), 841-854 (2021).
39. Sahibzada MU, Sadiq A, Khan S, Faidah HS, Naseemullah, Khurram M, Amin MU, Haseeb A.

Fabrication, characterization and in vitro evaluation of silibinin nanoparticles: an attempt to enhance its oral bioavailability. Drug Design, Development, and Therapy, 11(2017), 1453-64 (2017).
40. U.S. P. XXII "US Pharmacopeial convention" Rockville, Md 1788-1789 (1990).
41. Wu JW, Lin LC, Hung SC, Chi CW, Tsai TH. Analysis of silibinin in rat plasma and bile for hepatobiliary excretion and oral bioavailability application. Journal of pharmaceutical and biomedicalanalysis, 45(4), 635-41 (2007).
42. Odiegwu CN, Chianella I, Azubike NC, Odiegwu UO, Ogbuowelu OS. Liver Function Test Values in Albino Wistar Rats Administered with Isolated Nigeria *Achatina achatina* Snail Lectin. GSC Biological and Pharmaceutical Sciences, 15(2), 92-102 (2021).
43. Roche Diagnostics. Blood Bilirubin and Transaminases Estimations on the Cobas C111System. Roche Diagnostics Gmbh, Sandhofer Strasse116, D-68305 Mannheim, Germany.2011.
44. Drury RA. A color Atlas of histological staining techniques. Journal of Clinical Pathology, 31(3), 298-298 (1978).
45. Di Costanzo A, Angelico R. Formulation strategies for enhancing the bioavailability of silymarin: the state of the art. Molecules, 24(11), 2155-83 (2019).
46. Németh Z, Csóka I, Semnani Jazani R, Sipos B, Haspel H, Kozma G, Kónya Z, Dobó DG. Quality by Design-Driven Zeta Potential Optimisation Study of Liposomes with Charge Imparting Membrane Additives. Pharmaceutics, 14(9), 1798-1822 (2022).
47. Mahapatra AP, Patil V, Patil R. Solubility enhancement of poorly soluble drugs by using novel techniques: A comprehensive review. International Journal of PharmTech Research, 13(2), 80-93 (2020).
48. Holder CF, Schaak RE. Tutorial on powder X-ray diffraction for characterizing nanoscale materials. Acs Nano, 13(7), 7359-65 (2019).
49. Tavano L, Alfano P, Muzzalupo R, de Cindio B. Niosomes vs microemulsions: new carriers for topical delivery of Capsaicin. Colloids and surfaces B: Biointerfaces, 87(2), 333-9 (2011).
50. Štukelj J, Svanbäck S, Agopov M, Löbmann K, Strachan CJ, Rades T, Yliruusi J. Direct measurement of amorphous solubility. Analytical chemistry, 91(11), 7411-7 (2019).
51. Bremmell KE, Prestidge CA. Enhancing oral bioavailability of poorly soluble drugs with mesoporous silica-based systems: Opportunities and challenges. Drug development and industrial pharmacy, 45(3), 349-58 (2019).
52. Kakran M, Sahoo NG, Li L, Judeh Z, Wang Y, Chong K, Loh L. Fabrication of drug nanoparticles by evaporative precipitation of nanosuspension. International journal of pharmaceutics,383(1-2), 285-92 (2010).
53. Albariqi AH, Chang RY, Tai W, Ke WR, Chow MY, Tang P, Kwok PC, Chan HK. Inhalable hydroxychloroquine powders for potential treatment of COVID-19. Journal of Aerosol Medicine andPulmonary Drug Delivery, 34(1), 20-31 (2021).
54. Yingchoncharoen P, Kalinowski DS, Richardson DR. Lipid-based drug delivery systems in cancer therapy: what is available and what is yet to come. Pharmacological Reviews, 68(3), 701-87 (2016).
55. Yousaf AM, Malik UR, Shahzad Y, Mahmood T, Hussain T. Silymarin-laden PVP-PEG polymeric composite for enhanced aqueous solubility and dissolution rate: preparation and in vitro characterization. Journal of Pharmaceutical Analysis, 9(1), 34-9 (2019).
56. Croissant JG, Butler KS, Zink JI, Brinker CJ. Synthetic amorphous silica nanoparticles: toxicity, biomedical and environmental implications. Nature Reviews Materials, 5(12), 886-909 (2020).
57. Ali I, Ullah S, Imran M, Saifullah S, Hussain K, Kanwal T, Nisar J, Shah MR. Synthesis of biocompatible triazole-based non-ionic surfactant and its vesicular drug delivery investigation. Chemistry and Physics of Lipids, 228(2020), 104894-104894 (2020).
58. Shah SM, Ullah F, Khan S, Shah SM, de Matas M, Hussain Z, Minhas MU, AbdEl-Salam NM, Assi KH, Isreb M. Smart nanocrystals of artemether: fabrication, characterization, and comparative in vitro and in vivo antimalarial evaluation. Drug design, development, and therapy,

10(2016), 3837-50 (2016).
59. Kayaert P, Van den Mooter G. Is the amorphous fraction of a dried nanosuspension caused by milling or by drying? A case study with Naproxen and Cinnarizine. European journal of pharmaceutics and biopharmaceutics, 81(3), 650-6 (2012).
60. Da Silva FL, Marques MB, Kato KC, Carneiro G. Nanonization techniques to overcome poor water-solubility with drugs. Expert opinion on drug discovery, 15(7), 853-64 (2020).
61. Chi Lip Kwok P, Chan HK. Nanotechnology versus other techniques in improving drug dissolution. Current pharmaceutical design, 20(3), 474-82 (2014).
62. Kumar M, Shanthi N, Mahato AK, Soni S, Rajnikanth PS. Preparation of luliconazole nanocrystals loaded hydrogel for improvement of dissolution and antifungal activity. Heliyon, 5(5), e01688-e01688 (2019).
63. Pestovsky YS, Martínez-Antonio A. "Gold Nanoparticles with Immobilized β-cyclodextrin-capsaicin Inclusion Complex for Prolonged Capsaicin Release." IOP Conference Series: Materials Science and Engineering, (Vol. 389, No. 1, p. 012030) (2018).
64. Upadhyay P, Bhattacharjee M, Bhattacharya S, Ahir M, Adhikary A, Patra P. Silymarin- loaded, lactobionic acid-conjugated porous PLGA nanoparticles induce apoptosis in liver cancer cells. ACS Applied Bio Materials, 3(10), 7178-92 (2020).
65. Piwowarczyk L, Kucinska M, Tomczak S, Mlynarczyk DT, Piskorz J, Goslinski T, Murias M, Jelinska A. Liposomal Nanoformulation as a Carrier for Curcumin and pEGCG—Study on Stabilityand Anticancer Potential. Nanomaterials, 12(8), 1274 (2022).
66. Pande VV, Abhale VN, Möschwitzer JP. Nanocrystal technology: a particle engineering formulation strategy for the poorly water-soluble drugs. International Journal of Pharmaceutics, 453(1), 126-41 (2016).
67. Voorhees PW. The theory of Ostwald ripening. Journal of Statistical Physics, 38(1/2), 231-52 (1985).
68. Kumar D, Lashari N, Ganat T, Ayoub MA, Soomro AA, Chandio TA. A review on applicationof nanoparticles in cEOR: Performance, mechanisms, and influencing parameters. Journal of Molecular Liquids, 353(2022), 118821 (2022).
69. Kaushik M, Niranjan R, Thangam R, Madhan B, Pandiyarasan V, Ramachandran C, Oh DH, Venkatasubbu GD. Investigations on the antimicrobial activity and wound healing potential of ZnO nanoparticles. Applied Surface Science, 479(2019), 1169-77 (2019).
70. Kesisoglou F, Panmai S, Wu Y. Nanosizing—oral formulation development and biopharmaceutical evaluation. Advanced drug delivery reviews. 2007 Jul 30;59(7):631-44.
71. Bhujbal SV, Mitra B, Jain U, Gong Y, Agrawal A, Karki S, Taylor LS, Kumar S, Zhou QT. Pharmaceutical amorphous solid dispersion: A review of manufacturing strategies. Acta Pharmaceutica Sinica B, 11(8), 2505-36 (2021).
72. Tvrdý V, Pourová J, Jirkovský E, Křen V, Valentová K, Mladěnka P. Systematic review of pharmacokinetics and potential pharmacokinetic interactions of flavonolignans from silymarin. Medicinal Research Reviews, 41(4), 2195-246 (2021).
73. Abdullah AS, Sayed IE, El-Torgoman AM, Kalam A, Wageh S, Kamel MA. Green Synthesisof silymarin–chitosan nanoparticles as a new nanoformulation with enhanced anti-fibrotic effects against liver fibrosis. International Journal of Molecular Sciences, 23(10), 5420-5420 (2022).
74. Pathak K, Raghuvanshi S. Oral bioavailability: issues and solutions via nanoformulations. Clinical pharmacokinetics, 54(4), 325-57 (2015).
75. Javed S, Kohli K, Ali M. Reassessing bioavailability of silymarin. Alternative medicine review, 16(3), 239-49 (2011).
76. Pradhan R, Lee DW, Choi HG, Yong CS, Kim JO. Fabrication of a uniformly sized fenofibrate microemulsion by membrane emulsification. Journal of Microencapsulation, 30(1), 42-8 (2013).
77. Sahibzada MU, Sadiq A, Zahoor M, Naz S, Shahid M, Qureshi NA. Enhancement of bioavailability and hepatoprotection by silibinin through conversion to nanoparticles prepared by theliquid antisolvent method. Arabian Journal of Chemistry, 13(2), 3682-9 (2020).

78. Hedaya M, Bandarkar F, Nada A. In vitro and in vivo evaluation of ibuprofen nanosuspensionsfor enhanced oral bioavailability. Medical Principles and Practice, 30(4), 361-8 (2021).
79. Sahibzada MU, Zahoor M, Sadiq A, ur Rehman F, Al-Mohaimeed AM, Shahid M, Naz S, Ullah R. Bioavailability and hepatoprotection enhancement of berberine and its nanoparticles prepared by the liquid antisolvent method. Saudi Journal of Biological Sciences, 28(1), 327-32 (2021).
80. Gupta R, Badhe Y, Mitragotri S, Rai B. Permeation of nanoparticles across the intestinal lipid membrane: dependence on shape and surface chemistry studied through molecular simulations. Nanoscale, 12(11), 6318-33 (2020).
81. Bhattacharyya J, Ahmed AB, Das S. Hepatoprotective function as well as solubility and oral bioavailability of nano-based silymarin: A potential review. International Journal of Pharmaceutical Sciences and Research, 12(10), 1000-11 (2021).
82. Yang KY, Hwang DH, Yousaf AM, Kim DW, Shin YJ, Bae ON, Kim YI, Kim JO, Yong CS, Choi HG. Silymarin-loaded solid nanoparticles provide excellent hepatic protection: physicochemicalcharacterization and in vivo evaluation. International journal of nanomedicine, 8(1), 3333-43 (2013).
83. Liang J, Liu Y, Liu J, Li Z, Fan Q, Jiang Z, Yan F, Wang Z, Huang P, Feng N. Chitosan-functionalized lipid-polymer hybrid nanoparticles for oral delivery of silymarin and enhanced lipid- lowering effect in NAFLD. Journal of Nanobiotechnology, 16(1), 1-2 (2018).
84. El-Nahas AE, Allam AN, Abdelmonsif DA, El-Kamel AH. Silymarin-loaded eudragit nanoparticles: formulation, characterization, and hepatoprotective and toxicity evaluation. AAPS Pharmscitech, 18(8), 3076-86 (2017).
85. Nasr SS, Nasra MM, Hazzah HA, Abdallah OY. Mesoporous silica nanoparticles, a safe optionfor silymarin delivery: Preparation, characterization, and in vivo evaluation. Drug Delivery and Translational Research, 9(5), 968-79 (2019).
86. Kumar N, Rai A, Reddy ND, Shenoy RR, Mudgal J, Bansal P, Mudgal PP, Arumugam K, Udupa N, Sharma N, Rao CM. Improved in vitro and in vivo hepatoprotective effects of liposomal silymarin in alcohol-induced hepatotoxicity in Wistar rats. Pharmacological Reports, 71(4), 703-12 (2019).
87. Poovi G, Damodharan N. Lipid nanoparticles: A challenging approach for oral delivery of BCS Class-II drugs. Future Journal of Pharmaceutical Sciences, 4(2), 191-205 (2018).
88. Mu H, Holm R. Solid lipid nanocarriers in drug delivery: characterization and design. Expert opinion on drug delivery, 15(8), 771-85 (2018).
89. EL Sayed HE, Morsy LE, Abo Emara TM, Galhom RA. Effect of carbon tetrachloride (CCl4)on the liver in adult albino rats: histological study. The Egyptian Journal of Hospital Medicine, 76(6), 4254-61 (2019).
90. Abdullah AS, El Sayed IE, El-Torgoman AM, Alghamdi NA, Ullah S, Wageh S, Kamel MA. Preparation and characterization of silymarin-conjugated gold nanoparticles with enhanced anti-fibrotic therapeutic effects against hepatic fibrosis in rats: role of MicroRNAs as molecular targets. Biomedicines, 9(12), 1767 (2021).
91. El Rabey HA, Rezk SM, Sakran MI, Mohammed GM, Bahattab O, Balgoon MJ, Elbakry MA, Bakry N. Green coffee methanolic extract and silymarin protect against CCl4-induced hepatotoxicityin albino male rats. BMC complementary medicine and therapies, 21(1), 1-11 (2021).
92. Clichici S, David L, Moldovan B, Baldea I, Olteanu D, Filip M, Nagy A, Luca V, Crivii C, Mircea P, Katona G. Hepatoprotective effects of silymarin coated gold nanoparticles in experimental cholestasis. Materials Science and Engineering: C, 115(2020), 111117 (2020).
93. Abdel-Wahhab MA, El-Nekeety AA, Salman AS, Abdel-Aziem SH, Mehaya FM, Hassan NS. Protective capabilities of silymarin and inulin nanoparticles against hepatic oxidative stress, genotoxicity and cytotoxicity of Deoxynivalenol in rats. Toxicon: Official Journal of the InternationalSociety on Toxinology, 142, 1-13 (2018).